

FSGS as an adaptive response to growth-induced podocyte stress

Ryuzoh Nishizono^{¶*}, Masao Kikuchi^{¶*}, Su Q. Wang[¶], Mahboob Chowdhury[¶], Viji Nair[¶], John Hartman[¶], Akihiro Fukuda^{¶*}, Larysa Wickman[£], Jeffrey B. Hodgin^{*}, Markus Bitzer[¶], Abhijit Naik[¶], Jocelyn Wiggins[¶], Matthias Kretzler[¶] and Roger C. Wiggins[¶]

Departments of Internal Medicine[¶], Pathology^{*}, and Pediatrics and Communicable Diseases[£], University of Michigan, Ann Arbor, MI 48103 and the First Department of Internal Medicine^{*}, University of Miyazaki, Miyazaki, Japan

Drs. Nishizono and Kikuchi contributed equally and are designated co-equal first authors.

Abstract

The mechanism of FSGS lesion development was evaluated using a transgenic (podocin promoter-AA-4E-BP1) rat in which podocyte capacity to hypertrophy in response to growth factor/nutrient signaling is impaired. FSGS lesions resembling human FSGS developed spontaneously by 7 months of age, and could be induced earlier by accelerating kidney hypertrophy by nephrectomy. Protection from FSGS lesion development was provided by three different interventions that had in common prevention of kidney growth and glomerular enlargement (calorie intake reduction, mTORC1 inhibition and ACE inhibition). Increased glomerular (but not podocyte) cell cycling was identified by Ki67 nuclear staining and unbiased transcriptomic analysis as necessary for FSGS lesion development. Early segmental glomerular lesions occurred in the absence of a detectable reduction in average podocyte number per glomerulus and resulted from individual glomerular capillary loops losing their podocytes. Therefore, in the face of rapid glomerular growth (cell cycling of non-podocyte glomerular cells)

podocytes are unable to divide and adapt adequately to cover some parts of the filtration surface. Parietal epithelial cell division, accumulation on Bowman's capsule, and tuft invasion occurred at these sites. The rat FSGS-associated transcriptomic signature correlated with human glomerular transcriptomes associated with progression, compatible with similar processes occurring in man. We conclude that FSGS lesion development resulted from glomerular growth that exceeded the capacity of podocytes to adapt. Modest modulation of the growth side of this equation significantly ameliorated progression, even when initiated late in the process. Glomerular growth itself is an under-appreciated therapeutic target for preservation of renal function.

Introduction

The podocyte depletion hypothesis posits that a mismatch between the glomerular filtration surface area to be served and the podocyte foot process coverage available in any individual glomerulus determines whether proteinuria and glomerulosclerosis supervene ^{1,2}. Relative podocyte depletion can be caused by a podocyte deficit (reduction in number, size or function), by enlargement of the glomerular filtration surface area, or by some combination of these mechanisms ³. The reason why glomerular sclerotic lesions are characteristically focal and segmental is not well understood.

In the podocin-AA-4E-BP1 transgenic Fischer344 rat every cell of the body except the podocyte has normal capacity to maintain structure/function and respond to growth signaling cues ¹. The intrinsic machinery of the podocyte itself is also normal in the sense that no rat protein is knocked down or genetically modified. The only abnormality present is that a modified version of the human 4E-BP1 protein of the mTORC1 pathway is expressed specifically by podocytes under the control of the human podocin promoter that becomes active in late glomerular development. The modified human 4E-BP1 protein used as a transgene has two threonine residues changed to alanine (AA-4EBP1) so that they cannot be phosphorylated. This prevents the mTORC1 kinase from

phosphorylating them as is necessary to release the CAP-binding protein eIF4e to initiate transcription. Expression of the AA-4E-BP1 transgene by podocytes thereby blunts the growth response to mTORC1 activation by growth factors and nutrients ^{4,5}. The intact homozygous transgenic (TG) rat at young age has normal appearing glomeruli, normal podocyte number, normal kidney function, grows normally and reproduces normally ¹. If one kidney is removed so that hypertrophic stress is imposed on the remaining kidney, podocytes are less able to cope with hypertrophic demand resulting in proteinuria and progression to end stage kidney disease over 12 weeks ¹. In this report we extend previous work to better understand the impact of various interventions on the development of FSGS lesion as well as investigate the mechanisms of FSGS development.

Results

Mature FSGS lesions in the AA-4E-BP1 transgenic rat. Homozygous male and female TG rats develop increased proteinuria by 7 months of age (300g body weight) by which time 16±7% of glomeruli contain typical mature FSGS lesions (Figure 1A) that closely resemble mature human FSGS lesions (Figure 1B). No increase in proteinuria or glomerulosclerosis occurs in wild type Fischer344 rats by 7 months of age ⁶ thereby confirming that FSGS lesion development is dependent on the transgene expressed specifically by podocytes.

Early FSGS lesion development. TG rats at 100g body weight have normal appearing glomeruli as judged by light microscopy (H and E, PAS and silver staining, Glepp1 immune-peroxidase) as well as by transmission and scanning electron microscopy ¹. If these 100g TG rats are nephrectomized in order to induce hypertrophy in the remaining kidney, by 3 weeks after nephrectomy the contralateral kidney has increased in weight by 63%, glomerular volume has increased by 48%, the urine protein:creatinine ratio has increased to 7.3, 15±8% of glomeruli

have developed segmental glomerular lesions as judged by Glepp1 immuno-peroxidase (Figure 1C), and 5% have developed adhesions to Bowman's capsule as detected by Masson Trichrome staining (Table 1). In association with 48% glomerular enlargement and development of FSGS lesions neither the average podocyte nuclear number per glomerulus nor the total podocyte volume per glomerulus (Glepp1 positive glomerular volume) has changed (Table 2), the rate of podocyte detachment measured in urine has not increased significantly (Table 1), and no free podocytes can be identified free in Bowman's space or in tubular lumens. Therefore, by 3 weeks after nephrectomy glomerular volume enlargement had not yet resulted in measurable podocyte loss. However, as a consequence of the glomerular volume enlargement and in association with FSGS lesion development in some glomeruli the podocyte nuclear density (number per volume) had decreased by 49.8% and the podocyte cell density (Glepp1 area density) had decreased by 30.3% while the average Glepp1 negative glomerular volume (representing the non-podocyte component of the glomerulus) had doubled (Table 2). In the early segmental lesions individual glomerular capillary loops (shown by the arrow in Figure 1C) have become completely devoid of their normal podocyte covering (as previously also noted by scanning electron microscopy ¹). No increased proteinuria and no FSGS lesions were observed in wild type rats subjected to the same hypertrophic stress conditions. Figure 1C also shows cells what appear to be parietal epithelial cells (PECs) accumulating on Bowman's capsule at the site of podocyte absence and invading the tuft. This is further supported by using Pax8 as a PEC marker and demonstrating similar accumulation of cells on Bowman's capsule adjacent to areas of segmental podocyte depletion (Figure 1D). In some glomeruli Pax8 positive cells can be seen within the podocyte-depleted regions of the glomerular tuft (Figure 1E).

Taken together these data support the hypothesis that in this model, nephrectomy resulted in compensatory glomerular enlargement that could not be accommodated by transgenic podocytes, thereby giving rise to naked glomerular capillary loops, proteinuria and accumulation of PECs

adjacent to areas of podocyte depletion that subsequently invade the tuft and will contribute to forming mature segmentally sclerotic lesions.

Prevention of FSGS lesion development by slowing glomerular growth rate. If the above hypothesis is correct then slowing the rate of growth of the glomerulus would be predicted to prevent FSGS lesion development. The mTORC1 complex senses and integrates growth factor signaling and nutrient supply (amino acids and glucose) that controls growth of cells and organs^{4,5}. As shown in Figures 2 and 3 slowing the rate of growth of the TG rat either by reducing calorie intake or by inhibiting the mTORC1 kinase pathway directly (by rapamycin) had identical effects to slow the rate of body weight gain, reduce kidney weight gain, reduce glomerular enlargement, prevent podocyte detachment measured in urine, prevent podocyte depletion from glomeruli, prevent proteinuria, prevent development of glomerulosclerosis and prevent reduction in renal function. This occurred in a dose-dependent fashion as shown by modest calorie intake reduction or lower dose rapamycin. This result confirms both the mTORC1-dependent and the growth-dependent nature of development of FSGS lesions and progression to ESKD in the model.

Supplementary Table 1 shows the effect of modulating individual components of the diet in the heterozygous fully grown transgenic rat. Protection of progression was achieved by 40%>20% calorie intake reduction and by low protein diet. High fat diet, possibly because it has low protein and carbohydrate content, was also partially protective, although this protection could be neutralized by adding extra carbohydrate in the form of 10% sucrose in the drinking water (to simulate the typical sucrose content of commercially available beverages). These data are compatible with the concept that hypertrophy-induced glomerular injury can be modulated by diets that effect energy sensing through the mTORC1 pathway.

Angiotensin II blockade also prevents kidney and glomerular growth and FSGS lesion development: Figure 4 shows that the ACE inhibitor enalapril did not slow body growth rate but did slow kidney growth rate and downstream consequences including glomerular volume

enlargement, proteinuria, increased rate of podocyte detachment, glomerular sclerosis and reduction in renal function. Enalapril also lowered blood pressure in the model. Thus angiotensin II blockade had the same effect on reducing kidney and glomerular growth and its downstream consequences as did calorie intake reduction and mTORC1 inhibition shown in Figures 2 and 3, but did not reduce the rate of body growth.

Timing of intervention: To simulate interventions in real life situations the three treatment strategies were initiated 3 weeks after nephrectomy at a time when the urine protein;creatinine ratio had reached a value of about 7 and early FSGS lesions were already present (Figure 5). Rapamycin (even at once per week dosing) was significantly effective, 20% calorie reduction alone was not significantly effective, and ACE inhibitor was significantly effective at reducing injury and proteinuria. The combination of modest 20% calorie reduction plus ACE inhibitor appeared to be more effective than either strategy alone.

Relationships of body weight, kidney weight and glomerular volume: Figure 6 shows how glomerular volume is related to kidney weight and body weight in the presence and absence of nephrectomy, and how these parameters are modulated by treatments that prevented development of FSGS. Glomerular volume is directly proportional to single kidney weight under all conditions tested including nephrectomy and sham nephrectomy (Figure 6A). There is also a linear relationship between single kidney weight and body weight as shown (Figure 6B). However, the steepness of the slope of this relationship depends on kidney mass. After removal of one kidney the slope relating body weight to kidney weight doubled such that for every incremental increase in body weight there was twice the increase in kidney weight (and therefore in glomerular volume). Therefore, body weight gain in the setting of reduced kidney mass imposes greater hypertrophic glomerular stress. The interventions that were protective of development of FSGS all modified the relationships such that the effect of nephrectomy on kidney weight gain in relation to body weight gain was reduced by about 50% (Figure 6C, D and E). The combination of ACE

inhibitor and moderate calorie restriction almost eliminated the accelerating effect of nephrectomy on kidney hypertrophy (Figure 6F).

Cell cycling: If glomerular growth is truly a key determinant of FSGS we would expect that cell cycling would be increased in non-podocyte cells of the glomerulus in association with glomerular enlargement. Accordingly, we performed Ki67 immunofluorescence to identify cells which had entered the cell cycle (Figure 1F and Table 3). Rats that developed FSGS lesions (TG.1K.ALD) had significantly increased rates of Ki67 positive cells in all kidney compartments examined, including in glomeruli. Sham-nephrectomized TG rats maintained on the *ad lib* diet (that did not develop FSGS lesions by 3 weeks after nephrectomy but did develop FSGS lesions by 7 months of age in the intact rat) also had increased intraglomerular Ki67 positive cells, although the number per glomerulus was less than in the nephrectomized rats that developed FSGS lesions by 3 weeks after nephrectomy. In contrast, conditions that prevented development of FSGS lesions (calorie intake reduction, rapamycin and ACE inhibition) were all associated with reduced rates of cell cycling in all kidney cortex compartments (i.e. growth was slowed). Parietal epithelial (PEC) Ki67 positive cells increased in rats that developed FSGS lesions, but not in other groups. These data are consistent with the growth data shown above and demonstrate that increased cell cycling is necessary, but not alone sufficient, for development of FSGS lesions in the model. If cell cycling was slowed by any of three mechanisms, then FSGS lesions did not occur in spite of nephrectomy.

Podocyte cell cycling: Podocyte cell cycling was assessed by a double label study using WT1 as a podocyte nuclear marker and Ki67 as a nuclear marker of cell cycling. In the TG.1K.ALD group that developed FSGS 57 glomeruli in 6 rats were imaged containing 787 WT1 positive nuclei and 534 Ki67 positive nuclei. One cell was identified with both a WT1 and Ki67 positive nucleus (<0.02% of Ki67 positive intraglomerular cells). Therefore, in spite of hypertrophic stress induced by nephrectomy that causes cell cycling in glomerular cells podocytes (as defined by WT1 positive nuclei) did not enter the cell cycle.

Transcriptomic signal associated with FSGS lesion development: To obtain an unbiased perspective of early events driving the FSGS phenotype we performed Affymetrix-based transcriptomic analysis of isolated glomerular RNA obtained 3 weeks after nephrectomy for the groups shown in Tables 1-3. To identify major pathways involved in FSGS lesion development we compared gene expression profiles from the group that developed FSGS lesions (TG.1K.ALD) to those that were prevented from developing FSGS lesions by treatments in spite of nephrectomy (TG.1K.CRD, TG.1K.ALD.Rapa and TG.1K.ALD.ACEi). Genes whose expression level changed significantly ($P < 0.05$) and in the same direction ($n=538$) were subjected to Ingenuity Canonical Pathway Analysis. The top 35 candidates in the Diseases or Functions Annotations were either “cell cycle” or various cancers. The top 4 candidates designated as various aspects of “cell cycle” are shown in Table 5, supporting the concept that differences in cell cycling was a major component of whether or not FSGS lesions occurred.

To compare the relative level of cell cycle gene expression in the different rat groups the G2M checkpoint was selected as a key cell cycle event. The HALLMARK_G2M_CHECKPOINT list of 200 genes from the Broad Institute was used to derive a score for each rat glomerular transcriptome as shown in Figure 7 (see methods). Both The TG and WT nephrectomized *ad lib* fed rat groups (TG.1K.ALD and WT.1K.ALD) had high G2M scores while TG nephrectomized rats treated to prevent FSGS development (TG.1K.CRD, TG.1K.ALD.Rapa and TG.1K.ALD.ACEi) had significantly lower scores. Non-nephrectomized TG and WT groups had intermediate scores. These data independently confirm the Ki67 data (Table 3), and again support the concept that high level cell cycling was necessary, but not sufficient, for FSGS lesion formation.

Podocyte transcriptomic signatures associated with FSGS development: If hypertrophic podocyte stress is indeed necessary for the FSGS phenotype under the conditions tested then this may be reflected in the podocyte transcriptomic signature. Table 4 provides parallel podometric and transcriptomic parameters for the different groups shown as a % of wild type rat

values. As noted above, podocyte number per glomerulus did not decrease in association with FSGS lesion development although podocyte density (measured by two different methods) did decrease due to increased non-podocyte cell cycling resulting in increased glomerular volume. As would be expected this podocyte “dilution” effect was also reflected by a significant reduction in podocyte-specific transcript expression as exemplified by WT1, podocin, nephrin and ptpro [Glepp1]) (Table 4). Therefore, podocyte transcript gene expression levels *per se* could not be interpreted as evidence of podocyte stress. However, differential podocyte expression of genes that are specific to the podocyte can be used to examine this question. Nephrin is preferentially down-regulated in stressed podocytes^{6,7}. The podocin:nephrin ratio increased significantly in association with FSGS lesion development in the TG.1K.ALD rat group that developed FSGS compared to other groups, compatible with podocyte hypertrophic stress occurring in association with FSGS lesion development.

Comparison of the rat FSGS transcriptomic signature to progressive human glomerular diseases transcriptomic signatures: If the gene expression signatures identified for rat FSGS lesion development do represent events taking place in association with progression in humans then we would expect that these altered patterns in gene expression might also be present in human progressive glomerular diseases. As shown in Table 6 a rat “FSGS gene expression signature” correlated highly with expression signatures for progressive human glomerular diseases reported in the Nephroseq database⁸.

Discussion

In the transgenic rat model acceleration of kidney growth rate (induced by contralateral nephrectomy) resulted in FSGS lesion development that progressed to ESKD within 12 weeks of nephrectomy. In contrast, slowing the kidney and glomerular growth rate by three different methods (calorie intake reduction, inhibiting the mTORC1 pathway [by rapamycin] or angiotensin

II blockade [by ACE inhibition] all prevented FSGS lesion development. The key impact of growth in non-podocyte glomerular cells was further confirmed by Ki67 analysis to quantitate cycling cells in various kidney compartments, and by unbiased glomerular transcriptomic analysis. In spite of a general increase in cell cycling mature podocytes themselves (identified by WT1 positive nuclei) did not enter the cell cycle. In parallel studies no FSGS lesions developed in wild type rats thereby demonstrating that podocyte susceptibility (conferred by the transgene) was also required for FSGS lesion development. We conclude that two different but complementary factors were both necessary for FSGS lesion development, although neither alone was sufficient. These are (i) enhanced cycling of glomerular cells (but not podocytes) under the influence of growth factors and nutrients that cause glomerular enlargement, and (ii) the inability of podocytes to adapt to these growth-induced stresses. Importantly, slowing the glomerular growth rate, even by quite modest amounts and after proteinuria was already present and when early FSGS lesions had already developed, slowed progression.

Across all mammalian species, from the smallest to the largest, body weight is directly proportional to glomerular volume ⁹. Similarly, glomerular volume increases in relation to body weight increase during normal growth ¹. Body weight is therefore a surrogate for glomerular volume, although, as shown in Figure 6, if nephron number (mass) becomes reduced for any reason (e.g. by 50% following nephrectomy) the relationship between rate of glomerular volume increase and weight gain doubles, thereby accounting for the increased podocyte hypertrophic stress that caused FSGS lesion development in the model system. Importantly, angiotensin II blockade prevented kidney weight increase, but not body weight increase, suggesting that normal kidney and glomerular growth both require angiotensin II while body growth as a whole does not. Angiotensin II blockade therefore serves to disassociate kidney growth and glomerular enlargement from body growth, thereby accounting for its protective effect. This effect of angiotensin II blockade parallels its' well-established role *in utero* where it retards normal fetal kidney growth and development ¹⁰.

Is this report relevant to FSGS as it occurs in man? The mature FSGS lesion in the rat model system was indistinguishable from a human FSGS lesion, and the rat FSGS-associated transcriptomic signature correlated with diverse progressive human glomerular diseases. Normal glomerular growth, particularly in the early years of life, requires podocytes to undergo remarkable size increases to maintain the filtration surface ¹¹. Although FSGS phenotypes represent a diverse collection of underlying genetic and other causes, they typically present to the clinician during phases of life associated with rapid body growth. This is strikingly apparent for early childhood and adolescence, but also occurs in adults in association with increased body size (large body size itself, obesity, acromegaly and dietary supplement intake and similar conditions) ¹². Indeed, the prevalence of FSGS has increased in parallel with the spread of the obesity epidemic first reported in the US and later observed in China, India, Brazil and elsewhere ¹²⁻²¹ in parallel with population access to essentially unlimited calorie intake and sedentary life-style that has impacted body size ²². The question of whether or not dietary intervention can slow the rate of CKD progression remains controversial although obesity is associated with worse outcome in all CKD, and bariatric surgery is shown to reduce proteinuria and slow the rate of kidney function decline ²³⁻²⁶. Growth factor overexpression drives glomerulosclerosis in model systems, although reported data from humans treated with exogenous growth factors is so far limited ²⁷. We focused on calorie intake since our prior work examined factors that impact the aging process where calorie intake reduction is well known to prolong life-span ^{6,28}. However, viewed through the prism of mTORC1 as the major transducer of growth signaling in all cells, one would expect that glucose, amino acids and growth factors would all be integrated through the mTORC1 pathway to drive growth and cell cycling in non-podocyte glomerular cells and thereby to promote podocyte hypertrophic stress, FSGS development and accelerated progression to ESKD in susceptible individuals.

The glomerulus is a complex machine containing several cell types each with common housekeeping and some more or less specific pathways that comprise its characteristic transcriptome. Therefore, interpretation of the global glomerular transcriptome in terms of

individual pathways is challenging. In this study an increase in the proportion of glomerular cells that were not podocytes resulted in a relative decrease in podocyte-specific transcripts (WT1, nephrin, podocin or ptpro [Glepp1]) even though the number of podocytes did not change measurably. These transcript changes *per se* therefore could not be interpreted as evidence of modulation of transcription by podocytes. In contrast, ratios of two podocyte-specific transcripts (e.g. podocin and nephrin) demonstrate that modulated transcription did occur in association with FSGS lesion development, as previously reported ^{6,7}.

From the FSGS mechanistic viewpoint glomerular enlargement in the TG rat model was associated with development of segmental lesions devoid of podocytes, as also occurs in man. At early time points these lesions could be seen to be related to glomerular capillary loops that had lost their podocyte covering as judged by both light microscopy and SEM ¹. At the same time the average number of podocytes per glomerulus was not measurably decreased and there was no increase in rate of podocyte detachment detected in the urine pellet. This is in contrast to the diphtheria toxin receptor model we previously reported where FSGS lesion development was driven specifically by podocyte loss ²⁹. Nagata and Kriz also reported FSGS lesion development in the absence of reduced podocyte number per glomerulus ³⁰.

What mechanisms could account for the observed segmental absence of podocytes apparently occurring without loss of podocytes from glomeruli? One possibility is that PECs invade the glomerular tuft and displace podocytes. In the model used podocyte-depleted tuft segments were present prior to and in the absence of invasion by Pax8 positive cells (PECs). Accumulation of PECs (some of which were Ki67 positive) occurred on Bowman's capsule opposite the podocyte-devoid tuft segments, and by the 3week time point in some glomeruli Pax8 positive cells had invaded podocyte-depleted areas. Therefore, in this model although PEC tuft invasion was not the primary initiator of FSGS lesion development, the data are entirely compatible with a model in which PECs play an essential role in driving FSGS lesion sclerosis as reported by Smeets,

Moeller and colleagues ³¹⁻³³. A second possibility is that podocytes detached from glomerular capillary loops in response to hypertrophic stress analogous to the “mitotic podocyte catastrophe” model suggested by Lasagni and colleagues ³⁴, and similar to what we previously observed in aging human glomeruli ³⁵. Although we were not able to identify detached podocytes in Bowman’s space or tubular lumens by histology or by urine podocyte assay and the podocyte number per glomerulus was not measurably decreased in association with FSGS lesion development, it is possible that the methods used were not sensitive enough to detect these events occurring in a subset of glomeruli. A third possibility is that in the setting of glomerular capillary loop enlargement that exceeds the capacity of podocytes to provide coverage the default response of the podocyte population is to cover whatever territory it can and abandon territory that cannot be covered. The capacity of mature podocytes to migrate is already demonstrated by several investigators ³⁶⁻³⁸. Under this “Abandoned Capillary Loop Hypothesis” it would make sense that the abandoned unit would be an individual capillary loop whose blood flow could be independently regulated to reduce protein loss. This hypothesis appears to best fit the data although further studies will be required to test it.

In summary, FSGS lesion development can be conceptualized as an adaptive glomerular response to the inability of one member of the glomerular team, the podocyte, to comply with the hypertrophic demand imposed by the other members of the glomerular team under the influence of nutrients and growth factors.

Concise Methods

Rat studies were approved by the University of Michigan Use and Care of Animals Committee (IACUC) (PRO00006209).

Reagents: GLEPP1 mouse monoclonal antibody (1B4) was raised against the recombinant rat GLEPP1 extracellular domain were used as described previously ³⁹. WT1 (SC-7385 monoclonal

IgG1) from Santa Cruz Biotechnology (Santa Cruz, CA), Phospho-S6 (no. 2215) from Cell Signaling Technology (Beverly, MA), Pax8 antibodies were purchased from Abcam, (Cambridge, MA) ab191870 rabbit monoclonal antibody, MHC Class II antibody from AbD Serotec (Raleigh, NC) MCA46GA mouse monoclonal antibody, and Ki67 from Novus biologicals (Littleton, CO) NB600-1252 rabbit monoclonal antibody.

Rat nephrectomy model: Wild type and transgenic Fischer344 rats (expressing the AA-4E-BP1 transgene under the control of the human podocin promoter) were used for study as previously reported ¹. Both homozygous and heterozygous transgenic rats were used for different studies. Male rats underwent nephrectomy or sham nephrectomy at 100g body weight. One day after nephrectomy they were placed on various interventions as outlined below. Rats were weighed once per week and one day per week they were placed into a metabolic cage for overnight (17hr) urine collection. In some experiments (Figures 2-5) rats were kept for 12-14 weeks after nephrectomy and then euthanized with perfusion-fixation of kidneys using PLP buffer (containing paraformaldehyde (2%), lysine (1.37%) and periodate (0.2%) at +4°C at 100 mmHg. In other experiments rats were kept for 3 weeks prior to euthanization with ketamine/diazepam and kidneys were harvested and weighed. Once per week body weight and blood pressure were measured and timed overnight urine collection for protein, creatinine, urea and urine mRNAs were collected.

FSGS prevention studies: On the day following nephrectomy 100g male rats were randomly assigned to various interventions. For calorie intake reduction studies rats were maintained in individual cages so that the amount of food delivered to each rat could be monitored. For all other studies rats were fed an ad lib regular chow diet. For mTORC1 inhibitor studies rapamycin (LC Laboratories, Woburn, MA) was dissolved in ethanol at 100 mg/mL and then diluted to 1 mg/mL in vehicle (distilled water containing 5% Tween-80 and 5% PEG). Rapamycin was delivered by intraperitoneal injection (10mg/kg in vehicle) every 2 days or once a week. Control rats received

vehicle alone. There were no differences noted between vehicle-treated and control *ad lib* fed rats. For ACE inhibitor studies enalapril (Sigma, St. Louis, MO) was delivered at 10 mg/kg/day in the drinking water as previously described ³⁹. Calorie reduction studies were performed as previously described using National Institute on Aging rat protocol (NIH31/NIA Fortified for CR feeding) and pellets as previously described ⁶ either as 40% calorie restriction or 20% calorie restriction. For other dietary studies the following diets were used: 6% protein diet (TD.90016), 40% protein diet (TD.90018) purchased from Harlan Laboratories, Madison, WI; and 45% fat diet (D12451) purchased from Research Diets Inc., New Brunswick, NJ. In some studies, sucrose 10% was added to drinking water to simulate the sugar content of Coca-Cola.

Histologic analysis: At nephrectomy 1mm slices of kidney were placed in 10% paraformaldehyde overnight and then soaked in 10% ethanol prior to storage and subsequent sectioning at 3um thickness for further study. Masson trichrome staining was performed for quantitation of adhesions and scarring by a blinded observer.

Podometric analysis: Immunofluorescence using WT1 monoclonal antibody in 3um thick paraformaldehyde-fixed sections was used to identify and measure podocyte nuclear number and size by ImagePro software in 25 consecutive glomerular tufts was performed as previously described ⁴⁰. True podocyte nuclear density and size was estimated using the quadratic equation developed to correct for section thickness and nuclear shape using a downloadable spread-sheet ⁴⁰. The coverslip of the immunofluorescently stained section was removed and the section restained by Glepp1 immunoperoxidase and counterstained by PAS. The % of the glomerular tuft that was Glepp1 positive representing podocytes in the same glomeruli imaged for WT1 podocyte nuclear counting was estimated using imaging software as previously described ⁴⁰. Average glomerular volume in the same 25 consecutive glomerular tuft profiles was estimated from the average glomerular tuft area using the method of Weibel as previously reported ^{12,40,41}. The proportion of tuft made up of podocytes was estimated by multiplying the average tuft volume by

the %glepp1 positive area. The podocyte nuclear number per tuft was estimated by dividing the average glomerular volume by the podocyte nuclear density. The average podocyte cell volume was estimated by dividing the total podocyte volume by the number of podocyte nuclei per glomerular tuft.

Ki67 analysis: Double immunofluorescent labelling using rabbit monoclonal antibody against Ki67 (red) and a mouse monoclonal antibody against Glepp1(green) with blue dapi staining was used identify dividing cells and glomerular and tubular structure in 3um paraformaldehyde-fixed sections. Compound images from the red, green and blue channels for 12 consecutive glomerular profiles were made for each rat at x20 magnification with a glomerulus in the center of the field. Ki67 positive cell nuclei in each cortical compartment were counted including parietal epithelial cells, podocytes, intraglomerular cells, periglomerular and interstitial cells and tubular cells. Averaged values for the 12 consecutive images were used for each rat. In parallel studies double label immunofluorescence performed using Ki67 (rabbit monoclonal) and WT1 (mouse monoclonal) to identify Ki67 positive podocytes. Class II immunofluorescence was also performed and quantitated as above.

Glomerular isolation: Rat glomeruli were isolated by sieving from kidney cortex derived from euthanized rats in which kidneys had been perfused phosphate buffered saline at 4°C. Purity of glomeruli was >95% and 98% of isolated glomeruli did not have Bowman's capsules. RNAlater was added to the glomerular preparation for storage at -80°C prior to RNA purification using the RNeasy kit. The quality of the purified RNA was >8 as judged by the RIN scale.

Transcriptomic studies: Preliminary studies showed that in adlib-fed transgenic rats by 3 weeks after nephrectomy there were only minor adhesions developed and glomeruli could be quantitatively isolated by sieving. Wild-type and transgenic rats at 100g were either nephrectomized or sham-nephrectomized. They were divided into 7 groups as shown in Tables 1-4. Specifically, the TG nephrectomized adlib fed group that developed FSGS lesions was

compared to the TG nephrectomized groups that were prevented from developing FSGS lesions by calorie intake reduction, rapamycin treatment or ACE inhibitor treatment. Three weeks after nephrectomy glomeruli were isolated from renal cortex by sieving. Rat Gene ST 2.1 Affymetrix gene arrays were developed by the University of Michigan Affymetrix Core. Genes that changed significantly ($P < 0.05$) in the same direction in all three prevention groups (TG.1K.CRD, TG.1K.ALD.Rapa and TG.1K.ALD.ACEi) compared to the group that developed FSGS (TG.1K.ALD) were identified ($n=538$). This gene list was used for Ingenuity Pathway Analysis as reported in the results to find that cell cycling was the major pathway common to all three treatment strategies for preventing FSGS. Transcriptomic data will be available through Nephroseq at the next iteration.

Transcriptomic scoring for comparison of cell cycle gene activity between groups: The HALLMARK_G2M_CHECKPOINT gene expression signature list of 200 genes associated with the G2/M cell cycle checkpoint was downloaded from the GSEA/MSigDB resource at the Broad Institute (<http://software.broadinstitute.org/gsea/msigdb>). Orthologues were found in the rat data set for 176 of these genes. An expression matrix was constructed from these genes across all samples which was then transformed using the singular value decomposition (SVD). The first principal component (PC1) of the resulting rotated matrix accounted for 46.6% of the total variance and correlated well ($r=0.80$) with the mean Z-normalized expression of member genes, and was thus selected to represent the signature over the sample space. The effective weighting of the component genes is implicitly non-uniform, with 16 of the 176 genes accounting for over 50% of the sum of squared weights and 44 genes for over 90%.

Urine processing and mRNA analysis: Rats were placed in freshly washed metabolic cages in which the collection pan had been rinsed with 100% ethanol as previously reported⁴². Food was removed. A timed overnight urine collection (average 17 hours) was collected into a plastic 50ml centrifuge tube. Urine (up to 50 ml in a sterile 50-ml plastic centrifuge tube) is centrifuged at 4°C

for 15 minutes at 4,000 rpm (3,200xg) on a table-top centrifuge. Two 2-ml aliquots of the supernatant were removed and stored at -20°C for protein, creatinine, and other measurements. The urine pellet was suspended in 750ul of cold diethylpyrocarbonate-treated PBS (pH, 7.4) at 4°C using a sterile disposable polystyrene transfer pipette and then transferred to a labeled 1.7-ml plastic centrifuge tube. A second 750ul of PBS was used to wash the bottom of the 50-ml centrifuge tube to recover any remaining pellet material, and added to the 1.7-ml tube. The transferred pellet material now in 1.5 ml PBS was then centrifuged at 12,000 rpm in a mini-centrifuge for 5 minutes at 4°C. The supernatant is discarded. To the centrifuged material (“washed” urine pellet) was added to 350 ul of RLT buffer containing β -mercaptoethanol at 10 ml/ml of RLT buffer according to the RNeasy Qiagen protocol (Germantown, MD). The pellet was suspended in RLT/ β -mercaptoethanol buffer and then frozen at -80°C for assay. RNA was purified by RNeasy column and reverse transcribed prior to assay using TaqMan primers for NPHS2 spanning exons 3-4 (Applied Biosystems cat. No. Rn00709834). A glomerular RNA preparation was used as a standard for every assay. Data were expressed per g of urine creatinine as arbitrary units.

Statistics: For rat studies shown in Figures 2-5 all results were presented as mean \pm SEM. For all other studies data are shown as the mean \pm 1SD. Means of variables in two or more independent groups were compared by the unpaired *t* test and ANOVA with Bonferroni correction.

Acknowledgements: RW acknowledges the support of the National Institutes of Health (grants R01 DK 46073 and R01 DK 102643 and the University of Michigan O’Brien Kidney Translational Core Center P30 DK081943. The content is the responsibility of the authors alone and does not necessarily reflect the views or policies of the Department of Health and Human Services, nor

does mention of trade names, commercial products or organizations imply endorsement by the U.S. government.

Statement of Competing Financial Interests: The authors have no competing financial interests.

References

1. Fukuda A, Chowdhury M, Venkatareddy M, Wang SQ, Nishizono R, Wickman L, Wiggins J, Muchayi T, Fingar D, Shedden K, Inoki K and Wiggins RC: Growth-dependent podocyte failure causes glomerulosclerosis. *J Am Soc Nephrol.* 23: 1351-63, 2012
2. Kriz W. Glomerular diseases: podocyte hypertrophy mismatch and glomerular disease. *Nat Rev Nephrol.* 2012 8:618-9
3. Wiggins R: The spectrum of podocytopathies: A unifying view of glomerular diseases. *Kidney Int* 71: 1205-1214, 2007
4. Dibble C and Manning B. Signal integration by mTORC1 coordinates nutrient input with biosynthetic output. *Nature Cell Biology* 15:555-564, 2013
5. Grahammer F, Wanner N, Huber TB. mTOR controls kidney epithelia in health and disease. *Nephrol Dial Transplant.* 29 Suppl 1:i9-i18, 2014
6. Wiggins J, Goyal M, Sanden S, Wharram B, Shedden K, Misek D, Kuick R, Wiggins RC. Podocyte hypertrophy, “adaptation” and “decompensation” associated with glomerular enlargement and glomerulosclerosis in the aging rat: Prevention by calorie restriction. *J Am Soc Nephrol* 16:2953-2966, 2005
7. Fukuda A, Wickman L, Venkatareddy M, Wang SQ, Chowdhury M, Wiggins J, Shedden K, Wiggins RC. Urine podocin:nephrin mRNA ratio as a podocyte stress biomarker. *Nephrology, Dialysis and Transplantation.* 27:4079-87, 2012
8. <https://www.nephroseq.org/>

9. Maluf N and Gassman J. Kidneys of the killerwhale and significance of reniculism. *Anat Record* 1998;250:34-44
10. Vinturache AE, Smith FG. Angiotensin type 1 and type 2 receptors during ontogeny: cardiovascular and renal effects. *Vascul Pharmacol.* 2014, 63:145-54
11. Kikuchi M, Wickman L, Rabah R and Wiggins RC. Podocyte number and density changes during early human life. *Pediatr Nephrol* 2016 Epub ahead of print.
12. D'Agati VD, Chagnac A, de Vries AP, Levi M, Porrini E, Herman-Edelstein M, Praga M. Obesity-related glomerulopathy: clinical and pathologic characteristics and pathogenesis. *Nat Rev Nephrol.* 2016 12:453-71
13. Bonilla-Felix M, Parra C, Dajani T, Ferris M, Swinford RD, Portman RJ, Verani R: Changing patterns in the histopathology of idiopathic nephrotic syndrome in children. *Kidney Int* 55: 1885–1890, 1999
14. Gulati S, Sharma AP, Sharma RK, Gupta A: Changing trends of histopathology in childhood nephrotic syndrome. *AmJ Kidney Dis* 34: 646–650, 1999
15. Braden GL, Mulhern JG, O'Shea MH, Nash SV, Ucci AA Jr, Germain MJ: Changing incidence of glomerular diseases in adults. *Am J Kidney Dis* 35: 878–883, 2000
16. Filler G, Young E, Geier P, Carpenter B, Drukker A, Feber J: Is there really an increase in non-minimal change nephrotic syndrome in children? *Am J Kidney Dis* 42: 1107–1113, 2003
17. Dragovic D, Rosenstock JL, Wahl SJ, Panagopoulos G, DeVita MV, Michelis MF: Increasing incidence of focal segmental glomerulosclerosis and an examination of demographic patterns. *Clin Nephrol* 63: 1–7, 2005
18. Swaminathan S, Leung N, Lager DJ, Melton LJ 3rd, Bergstralh EJ, Rohlinger A, Fervenza FC: Changing incidence of glomerular disease in Olmsted County, Minnesota: A 30-year renal biopsy study. *Clin J Am Soc Nephrol* 1: 483–487, 2006

19. Borges FF, Shiraichi L, da Silva MP, Nishimoto EI, Nogueira PC: Is focal segmental glomerulosclerosis increasing in patients with nephrotic syndrome? *Pediatr Nephrol* 22: 1309–1313, 2007
20. Zhou FD, ZhaoMH, ZouWZ, Liu G, Wang H: The changing spectrum of primary glomerular diseases within 15 years: a survey of 3331 patients in a single Chinese center. *Nephrol Dial Transplant* 24: 870–876, 2009
21. Das U, Dakshinamurty KV, Prayaga A: Pattern of biopsy-proven renal disease in a single center of south India: 19 years of experience. *Indian J Nephrol* 21: 250–257, 2011
22. Finucane MM, Stevens GA, Cowan MJ, Danaei G, Lin JK, Paciorek CJ, Singh GM, Gutierrez HR, Lu Y, Bahalim AN, Farzadfar F, Riley LM, Ezzati M; Global Burden of Metabolic Risk Factors of Chronic Diseases Collaborating Group (BodyMass Index): National, regional, and global trends in body-mass index since 1980: Systematic analysis of health examination surveys and epidemiological studies with 960 country years and 9.1 million participants. *Lancet* 377: 557–567, 2011
23. Clase CM, Smyth A. Chronic kidney disease. *BMJ Clin Evid*. 2015 Jun29; pii:2004.
24. Nehus EJ, Khoury J, Inge T, Xiao N, Jenkins T, Moxey-Mims M, Mitsnefes M. Kidney outcomes three years after bariatric surgery in severely obese adolescents. *Kidney Int*. 2016 E-pub.
25. Li K, Zou J, Ye Z, Di J, Han X, Zhang H, Liu W, Ren Q, Zhang P. Effects of Bariatric Surgery on Renal Function in Obese Patients: A Systematic Review and Meta-Analysis. *PLoS One*. 2016;11:e0163907
26. Nehus E, Khoury J, Inge T, Xiao N, Jenkins T, Moxey-Mims M, Mitsnefes M. Kidney outcomes three years after bariatric surgery in severely obese adolescents *Kidney Int* 2017 91:451-458

27. Doublier S, Seurin D, Fouqueray B, Verpont MC, Callard P, Striker LJ, Striker GE, Binoux M, Baud L. Glomerulosclerosis in mice transgenic for human insulin-like growth factor-binding protein-1. *Kidney Int.* 2000 Jun;57(6):2299-307
28. Wiggins JE, Patel S, Shedden K, Goyal M, Wharram B, Martini S, Kretzler M, Wiggins RC: NFkB in the pro-inflammatory, pro-coagulant, pro-fibrotic aging glomerulus. *J Am Soc Nephrol.* 2010, 21:587-97
29. Wharram BL, Goyal M, Gillespie PJ, Wiggins JE, Kershaw DB, Holzman LB, Dysko RC, Saunders TL, Samuelson LC, Wiggins RC: Podocyte depletion causes glomerulosclerosis: Diphtheria toxin-induced podocyte depletion in rats expressing human diphtheria toxin receptor transgene. *J Am Soc Nephrol* 16: 2941-2952, 2005
30. Nagata M and Kriz W. Glomerular damage after uninephrectomy in young rats. II. Mechanical stress on podocytes as a pathway to sclerosis. *Kidney Int* 42:148-160, 1992
31. Smeets B, Kuppe C, Sicking EM, Fuss A, Jirak P, van Kuppelvelt TH, Endlich KH, Wetzels JF, Grone HJ, Floege J, and Moeller MJ: Parietal epithelial cells participate in the formation of sclerotic lesions in focal and segmental glomerulosclerosis (FSGS). *J Am Soc Nephrol* 22: 1262-74, 2011
32. Smeets B, Stucker F, Wetzels J, Brocheriou I, Ronco P, Gröne HJ, D'Agati V, Fogo AB, van Kuppevelt TH, Fischer HP, Boor P, Floege J, Ostendorf T, Moeller MJ. Detection of activated parietal epithelial cells on the glomerular tuft distinguishes early focal segmental glomerulosclerosis from minimal change disease. *Am J Pathol.* 2014 184:3239-48.
33. Kuppe C, van Roeyen C, Leuchtle K, Kabgani N, Vogt M, Van Zandvoort M, Smeets B, Floege J, Gröne HJ, Moeller MJ. Investigations of Glucocorticoid Action in GN. *J Am Soc Nephrol.* 2016 Nov 28. pii: ASN.2016010060. [Epub ahead of print]
34. Lasagni L, Lazzeri E, Shankland S, Anders H, Romagnani P. Podocyte mitosis - a catastrophe. *Curr Mol Med* 2013;13:13-23

35. Hodgin J, Bitzer M, Wickman L, Afshinnia F, Wang S, Yang Y, Meadowbrooke C, Chowdhury M, Kikuchi M, Wiggins J, Wiggins RC. Kidney aging and Focal Global Glomerulosclerosis. A podometric perspective. *J Am Soc Nephrol.* 2015;26:3162-78
36. Hackl MJ, Burford JL, Villanueva K, Lam L, Suszták K, Schermer B, Benzing T, Peti-Peterdi J. Tracking the fate of glomerular epithelial cells in vivo using serial multiphoton imaging in new mouse models with fluorescent lineage tags. *Nat Med.* 2013 12:1661-6
37. Schulte K, Berger K, Boor P, Jirak P, Gelman IH, Arkill KP, Neal CR, Kriz W, Floege J, Smeets B, Moeller MJ. Origin of parietal podocytes in atubular glomeruli mapped by lineage tracing. *J Am Soc Nephrol.* 2014, 25:129-41
38. Lasagni L, Angelotti ML, Ronconi E, Lombardi D, Nardi S, Peired A, Becherucci F, Mazzinghi B, Sisti A, Romoli S, Burger A, Schaefer B, Buccoliero A, Lazzeri E, Romagnani P. Podocyte Regeneration Driven by Renal Progenitors Determines Glomerular Disease Remission and Can Be Pharmacologically Enhanced. *Stem Cell Reports.* 2015, 5:248-63.
39. Fukuda A, Wickman LT, Venkatareddy MP, Sato Y, Chowdhury MA, Wang SQ, Shedden KA, Dysko RC, Wiggins JE, Wiggins RC: Angiotensin II-dependent persistent podocyte loss from destabilized glomeruli causes progression of end stage kidney disease. *Kidney Int* 81: 40-55, 2012
40. Venkatareddy M, Wang SQ, Yang Y, Patel S, Wickman L, Nishizono R, Chowdhury M, Hodgin J, Wiggins PA and Wiggins RC Estimating podocyte number and density in histologic sections. *J Am Soc Nephrol.* 25:1118-1129, 2014
41. Weibel ER. Stereologic methods: Practical methods for biologic morphometry: London, Academic Press, Inc., pp40-116, 415. 1979
42. Sato Y, Wharram BL, Lee SK, Wickman L, Goyal M, Venkatareddy M, Chang JW, Wiggins JE, Lienczewski C, Kretzler M, Wiggins RC. Urine podocyte mRNAs mark progression of renal disease. *J Am Soc Nephrol.* 2009 20:1041-52.

Figure Legends

Figure 1. Anatomic features of the FSGS lesion. Panel A. Transgenic rat glomerulus showing a mature FSGS lesion at 7 months by glepp1 peroxidase counter-stained with PAS. Podocytes are absent from the sclerotic area (arrowhead) in contrast to the remainder of the tuft which shows a normal distribution of brown peroxidase positive Glepp1-stained podocytes (arrow). An adhesion joining Bowman's capsule to the glomerular tuft is also present (fluted arrowhead). **Panel B. A mature human FSGS lesion that is identical to the rat FSGS lesion shown in Panel 1A.** The arrows point to the same features as emphasized for Figure 1A. **Panel C. Early segmental FSGS lesion present at 3 weeks after nephrectomy of the AA-4E-BP1 rat model.** A naked glomerular capillary loop (arrow) is devoid of the brown-staining Glepp1-peroxidase product that is present in the remaining tuft area (arrowhead). Parietal epithelial cells (PECs) accumulate on Bowman's capsule adjacent to the segmental lesion and some PECS appear to have invaded the tuft within the segmental lesion. **Panel D and E. Parietal epithelial cells (PECs), identified by their pink Pax8 positive nuclei.** In Panel D Pax8 positive cells have accumulated opposite an early developing FSGS lesion that is losing its podocytes (as indicated by loss of green Glepp1-stained cytoplasm). In Panel E the Pax8 positive PECs are invading the glomerular tuft at a site of absent podocytes (as shown by absence of Glepp1 green fluorescence). Nuclei are shown by blue DAPI staining. **Panel F. Ki67 immunofluorescence to identify dividing cells.** In association with development of the early FSGS lesion as indicated by loss of Glepp1 positive green signal, Ki67 positive nuclei representing cycling cells (pink nuclei) are present on Bowman's capsule (PECs), within the glomerular tuft (intrinsic glomerular cells), in the peri-glomerular and interstitial compartments, and in tubules. Double labelling studies for WT1 and Ki67 showed no double positive cells indicating that cells identified as podocytes on the basis of anatomical location were not WT1 positive podocytes. Class II staining showed no increase in class II positivity in association with FSGS lesion formation.

Figure 2: Dietary calorie intake reduction prevents growth-induced glomerular failure in the AA-4E-BP1 model in a dose-dependent manner. Dietary calorie intake reduction (40% reduction>20% reduction) has the following protective effects: Body weight gain was slowed (**A**); Kidney weight gain was reduced; (**F**) Glomerular tuft volume was reduced (**I**); Rate of podocyte detachment was reduced (**D**); Reduction of podocyte number per glomerular tuft was prevented (**K**); Reduction in podocyte density was prevented (**L**); The increase in podocyte cell volume was prevented (**J**); Urine protein:creatinine ratio was reduced (**C**); Percent of glomeruli with adhesions and amount of glomerulosclerosis were reduced (**G and E1,2 and 3**); Decreased creatinine clearance was prevented (**H**); Systolic blood pressure increase with age was prevented (**B**). Data shown as the mean \pm the SEM. * = P<0.05, ** = P<0.01.

Figure 3: The mTORC1 inhibitor rapamycin prevents growth-induced glomerular failure in the AA-4E-BP1 model. Rapamycin (delivered at 10mg/kg by IP injection on alternate days [dark green line] or at low dose once per week [light green line]) inhibited mTORC1 kinase activity as demonstrated by completely preventing phosphorylation of ribosomal S6 in glomeruli and tubules shown by green immunofluorescence (**E1 versus E2**). Podocytes are shown by red WT1 immunofluorescent staining. In contrast lower dose rapamycin (delivered as 10mg/kg by IP injection once per week) did not fully inhibit ribosomal S6 phosphorylation (**E1 versus E3**). Rapamycin treatment had the following protective effects: Body weight gain was slowed (**A**); Kidney weight gain was reduced; (**F**) Glomerular tuft volume was reduced (**I**); Rate of podocyte detachment was reduced (**D**); Reduction of podocyte number per glomerular tuft was prevented (**K**); Reduction in podocyte density was prevented (**L**); There was no significant change in podocyte cell volume (**J**); Urine protein:creatinine ratio was reduced (**C**); Percent of glomeruli with adhesions and amount of glomerulosclerosis were reduced (**G**); Decreased creatinine clearance was prevented (**H**); Systolic blood pressure increase with age was not prevented (**B**). Data shown as the mean \pm the SEM. * = P<0.05, ** = P<0.01.

Figure 4: ACE inhibition prevented growth-induced glomerular failure in the AA-4E-BP1 model. The following protections were observed by ACE inhibitor treatment with enalapril (10mg/kg/day in the drinking water): Body weight gain was not changed (**A**); Kidney weight gain was reduced; (**F**) Glomerular tuft volume was reduced (**I**); Rate of podocyte detachment was reduced (**D**); Reduction of podocyte number per glomerular tuft was prevented (**K**); Reduction in podocyte density was prevented (**L**); The increase in podocyte cell volume was not significantly reduced (**J**); Urine protein:creatinine ratio was reduced (**C**); Percent of glomeruli with adhesions and amount of glomerulosclerosis were reduced (**G and E1 and 2**); Decreased creatinine clearance was prevented (**H**); Systolic blood pressure increase with age was prevented (**B**). Data shown as the mean \pm the SEM. * = $P < 0.05$, ** = $P < 0.01$.

Figure 5: Later intervention 3 weeks after nephrectomy when the urine protein:creatinine ratio was 10 was partially effective in preventing growth-induced glomerular failure in the AA-4E-BP1 model. Rapamycin (10mg/kg by IP injection) was started either on day 1 (solid green line) or day 21 (dotted green line or striped bar) after nephrectomy. Modest 20% calorie reduction was started either on day 1 (solid blue line) or day 21 (dotted blue line or striped bar) after nephrectomy. ACE inhibitor (enalapril at 10mg/kg/day) was started either on day 1 (solid red line) or day 21 (dotted red line or striped bar) after nephrectomy. The combination of calorie reduction (20%) and ACE inhibitor (enalapril 10mg/kg/day) was started either on day 1 (solid purple line) or day 21 (dotted purple line or striped bar) after nephrectomy. Data are shown for the urine protein:creatinine ratio (**A**), the kidney weight (**B**) and % of glomeruli with adhesions (**C**). In each case the later intervention was less effective than the earlier intervention at preventing kidney weight change and glomerular injury. Modest calorie intake reduction in combination with ACE

inhibition appeared more effective than either treatment alone. Data shown as the mean \pm the SEM. * = $P < 0.05$, ** = $P < 0.01$.

Figure 6: Relationship between glomerular volume, kidney weight and body weight. Panel

A. Glomerular volume was directly proportional to kidney weight under all conditions and diets tested. Kidney weight (mass) is therefore a surrogate for glomerular volume. **Panel B.** As previously reported (7) the slope of the relationship between single kidney weight (SKW) and body weight (BW) doubles when one kidney is removed (2K to 1K), and the SKW:BW ratio relationship remains constant as the animal continues to increase weight thereby creating increased podocyte hypertrophic stress after nephrectomy. **Panel C.** Rapamycin reduced the slope SKW:BW ratio by about 50%. SKW is therefore preferentially reduced compared to BW by mTORC1 inhibition. **Panel D.** Calorie reduction (CR) reduced the SKW:BW ratio in relation to the degree of calorie reduction (40% CR (open squares) >20% CR (open diamonds)). SKW is therefore also preferentially reduced compared to BW by CR. **Panel E.** ACE inhibitor (ACEi) reduced the SKW:BW ratio by about 50%. SKW is therefore again preferentially reduced compared to BW by ACE inhibitor treatment. **Panel F.** The combination of CR and ACEi (10mg/kg/day) reduced the SKW:BW ratio almost back to the normal 2K state.

Figure 7. Glomerular transcriptional HALLMARK_G2M_CHECKPOINT cell cycle signature

for rat groups. Each rat glomerular Affymetrix transcriptome was used to obtain a G2M signature value derived from the “Hallmark_G2M” gene list downloaded from the GSEA/MSigDB molecular signatures database at the Broad Institute (see methods). Data was normalized as shown on the y axis. Individual points for each rat are shown according to groupings defined according to whether they were TG or WT, nephrectomized (1K) or sham-nephrectomized (2K0), and whether they were maintained on an ad lib diet (ALD) or a calorie intake reduction diet (CRD). Data for groups are shown as box plots with a mean and interquartile range. The rat group that developed FSGS lesions (TG.1K.ALD) was significantly different from all groups ($P < 0.01$) except the

WT.1K.ALD group. TG rat groups that were prevented from developing FSGS in spite of undergoing nephrectomy (TG.1K.ALD, TG.1K.ALD.Rapa and TG.1K.ALD.ACEi) had significantly lower G2M values. Note that 98% of glomeruli purified by sieving for Affymetrix analysis do not include Bowman's capsule and therefore PECs are not represented. The group distribution is similar to the Ki67 data shown in Table 3.

Table 1

Groups	Body weight g	Kidney weight g	Urine protein:creatinine ratio	Serum creatinine mg%	Adhesions %	Urine podocin mRNA:creat ratio units/g creatinine
TG.1K.ALD (FSGS)	202±7	1.8±0.2	7.3±1.6	1.4±0.1	5.6±2.6	3.1±2.1
TG.2K.ALD	202±15	1.1±0.2**	2.4±0.5**	1.1±0.2	0.0**	0.7±0.3
TG.1K.CRD	144±9**	0.9±0.1**	0.9±0.3**	1.3±0.2	0.0**	1.1±0.2
TG.1K.ALD.Rapa	145±9**	1.1±0.1**	1.1±0.1**	1.7±0.3	0.0**	0.3±0.2*
TG.1K.ALD.ACEi	196±8	1.3±0.1**	1.4±0.2**	1.4±0.2	0.0**	4.4±3.3

Table 1 legend: Phenotyping for TG rat groups 3 weeks after nephrectomy or sham nephrectomy). Data for the control group prior to surgery at time 0 is shown at top. The remaining groups were evaluated 3 weeks after surgery (n=5-7 per group). FSGS with adhesions to Bowman's capsule identified on Masson trichrome-stained sections was observed only in the nephrectomized ad lib-fed group and was associated with greater kidney weight gain and higher level proteinuria. FSGS lesions did not develop if rats did not undergo nephrectomy that caused compensatory kidney hypertrophy, or were prevented from gaining body weight by either calorie reduction or rapamycin treatment, or were treated with ACE inhibitor that did not prevent body weight gain but did prevent kidney enlargement. The rate of podocyte detachment as measured by the urine podocin mRNA:creatinine ratio was not significantly increased by 3 weeks in any group. The statistical comparisons shown compare the four groups that did not develop FSGS to the nephrectomized ad lib fed group that did develop FSGS. Statistical

comparisons by ANOVA with Bonferroni correction. * = $P < 0.05$, ** = $P < 0.01$. TG=transgenic rats, 1K/2K=nephrectomized/sham-nephrectomized, ALD=adlib diet, CRD=40% calorie reduced diet, rapa=rapamycin-treated, ACEi=treated with angiotensin II inhibitor enalapril.

Table 2

Group	Glomerular volume $\times 10^6 \text{ um}^3$	Podocyte # per tuft n	Podocyte nuc density per 10^6 um	Podocyte volume $\times 10^3 \text{ um}^3$	Glepp1 area %	Glepp1 +ve glom vol $\times 10^3 \text{ um}^3$	Glepp1 -ve glom vol $\times 10^3 \text{ um}^3$
TG.1K.ALD (FSGS)	1.2±0.1	145±15	120±11	2.7±0.2	32.6±2.7	379±80	817±105
TG.2K.ALD	0.8±0.2**	142±31	178±38**	2.7±0.5	46.7±1.5**	393±46	429±78**
TG.1K.CRD	0.7±0.2**	146±21	212±21**	2.1±0.2*	44.7±2.3**	313±68	392±110**
TG.1K.ALD.Rapa	0.5±0.1**	126±19	248±15**	1.8±0.1**	44.2±1.3**	225±25**	285±43**
TG.1K.ALD.ACEi	0.8±0.1**	131±17	212±29*	2.7±0.4	41.8±1.4**	345±40	483±81**
WT.2K.ALD	0.6±0.1**	130±19	241±73**	2.1±0.6	46.8±1.6**	271±43	263±51**
WT.1K.ALD	0.6±0.1**	136±19	272±73**	1.9±0.7	46.8±1.1**	252±50	309±45**

Table 2 legend: Podometric analysis for TG or WT rat groups 3 weeks after nephrectomy (1K) or sham nephrectomy (2K). All groups (n=5-7) were evaluated 3 weeks after surgery. Statistical comparisons by ANOVA with Bonferroni correction (* = P<0.05, ** = P<0.01) are shown for all groups in comparison to the nephrectomized ad lib-fed group that developed FSGS (TG.1K.ALD) (top row). There was no reduction

in podocyte number per glomerulus in TG.1K.ALD rats that developed FSGS. On the other hand, the glomerular volume was increased resulting in reduced podocyte nuclear density and Glepp1 area density and an increase in the Glepp1 negative (non-podocyte) glomerular volume compared with other groups. Prevention of FSGS by calorie reduced diet (CRD), rapamycin (Rapa) or ACE inhibitor were all associated with maintenance of smaller glomerular volume and higher podocyte nuclear density and Glepp1 area density. WT nephrectomized or sham-nephrectomized rats on an ad lib diet did not develop increased proteinuria or FSGS lesions and maintained podometric values that were not significantly different from the TG sham-nephrectomized group that did not develop FSGS. Abbreviations as follows: TG, Fischer344 transgenic rats; WT, wild type Fischer344 rats; 1K/2K, nephrectomized/sham-nephrectomized; ALD, adlib diet; CRD, 40% calorie reduced diet; rapa, rapamycin-treated; ACEi, treated with the angiotensin II inhibitor enalapril.

Table 3

Group	Ki67 positive nuclei per field				
	Intraglomerular	Podocyte	PEC	Periglomerular /Interstitial	Tubular
TG.1K.ALD (FSGS)	10.3±1.7**	0.01±0.1	2.8±0.7**	8.2±2.2**	4.0±1.1**
TG.2K.ALD	6.4±0.9**	0.1±0.1	0.9±0.4	3.2±0.5	2.0±0.4
TG.1K.CRD	1.9±1.2	0.0±0.0	0.6±0.3	1.7±0.9	0.7±0.4
TG.1K.ALD.Rapa	2.0±1.2	0.0±0.0	0.4±0.2	2.3±0.8	1.1±0.7
TG.1K.ALD.ACEi	2.8±0.6	0.0±0.0	0.7±0.3	2.7±1.0	1.3±0.5
WT.2K.ALD	4.5±1.0**	0.0±0.0	0.7±0.4	3.2±0.8	2.5±0.9
WT.1K.ALD	6.7±1.0*	0.0±0.0	0.6±0.3	2.6±0.2	2.8±1.1

Table 3 legend: Ki67 positive cell nuclei in different kidney compartments in nephrectomized (1K) or sham-nephrectomized (2K) TG and WT rat groups under different conditions. Group descriptors (n=5-7) are shown at left. Statistical indicators using ANOVA with Bonferroni adjustment (*P<0.05, **P<0.01) compare each group with the reduced calorie intake group (TG.1K.CRD). All rats were the same age, weight and sex at start of study 3 weeks prior to analysis. There were no changes in podocyte Ki67 positive nuclei in any group, and in a

parallel study, no Ki67 cell nuclei were identified that were also WT1 positive (data not shown) and no binucleate WT1 positive cells were identified indicating that cells designated as podocytes on the basis of their anatomic localization were probably PECs. In the TG.1K.ALD group that developed FSGS (top row) Ki67 positive nuclei were statistically increased in all other kidney compartments. In the Sham nephrectomized TG group (TG.2K.ALD) and WT nephrectomized and sham-nephrectomized groups only intraglomerular Ki67 positive cells were significantly increased above the reduced calorie intake (TG.1K.CRD) group, but these three groups also had significantly fewer intraglomerular Ki67 positive cells than the TG.1K.ALD (FSGS) group ($P < 0.01$). Prevention of FSGS development by three different methods (CRD, Rapamycin or ACE inhibition) all showed the similar Ki67 data demonstrating low cell division in all kidney compartments indicating that cell division rate was similarly slowed by all three strategies. These data are consistent with the concept that growth represented by Ki67 positive cells was required for FSGS development. If cell division/growth was prevented (by calorie reduction, rapamycin or ACE inhibitor) or was not sufficiently rapid (sham-nephrectomy), or the susceptibility transgene was absent (WT rats) FSGS did not occur within the 3week time frame of study. Statistical comparisons by ANOVA with Bonferroni correction. * = $P < 0.05$, ** = $P < 0.01$. Abbreviations as follows: TG, Fischer344 transgenic rats; WT, wild type Fischer344 rats; 1K/2K, nephrectomized/sham-nephrectomized; ALD, adlib diet; CRD, 40% calorie reduced diet; rapa, rapamycin-treated; ACEi, treated with the angiotensin II inhibitor enalapril.

Table 4

	Podometric parameters			Glomerular transcript values expressed as % compared to WT.2K.ALD				
	Podocyte number per glom	Podocyte nuclear density	Glepp1 area density	WT1	Podocin	Nephrin	Ptpro (Glepp1)	Podocin: Nephrin Ratio
TG.1K.ALD	106.6±10.7	49.9±4.7**	69.6±5.8**	60.3±13.1**	67.6±11.1*	50.8±9.4**	51.6±8.1**	132.7±3.2**
TG.2K.ALD	104.5±23.0	74.0±15.9	99.8±3.1	107.1±17.8	99.5±16.0	93.0±14.5	121.5±16.4	106.5±4.0
TG.1K.CRD	107.4±15.7	87.9±12.0	95.5±4.8	101.1±18.5	83.6±14.9	87.9±15.4	91.4±12.2	94.8±8.9
TG.1K.ALD.Rapa	92.9±13.8	102.7±6.4	94.5±2.7	30.4±10.1**	33.1±9.0**	24.3±8.9**	34.5±11.9**	140.9±18.5**
TG.1K.ALD ACEi	96.1±12.2	76.6±13.8	89.4±3.1	68.3±13.4*	66.4±14.5*	62.4±12.1**	63.9±13.4**	105.4±7.0
WT.1K.ALD	95.8±14.0	113±31.2	99.9±2.4	88.7±4.5	94.9±5.3	86.9±6.7	77.9±9.6	108.9±3.5
WT.2K.ALD	100±14.0	100±30.2	100±3.4	100±11.7	100±5.7	100±13.0	100±8.0	100±8.5

Table 4 Legend. Comparison of glomerular podometric and transcriptomic parameters. All data are from isolated glomeruli obtained 3 weeks after nephrectomy or sham nephrectomy for the same groups as shown in Table 1-3. Data shown in comparison with the wild type sham-nephrectomized rats maintained on an ad lib diet (WT.2K.ALD in bottom row at 100%). Podometric parameters are shown at left, relative transcriptomic expression in the middle, and podocyte transcript ratios at right. Nephrectomized transgenic rats maintained on an ad lib diet (TG.1K.ALD) that developed FSGS are shown in the top row. In this group, although podocyte number per glomerulus was unchanged,

podocyte nuclear density and Glepp1 cell area density were both decreased due to glomerular enlargement partially compensated for by podocyte cell hypertrophy. Podocyte transcripts (WT1, podocin, nephrin and ptpo (Glepp1) were all decreased in approximate proportion to the decreased podocyte density. In contrast desmin transcript, which increases in stressed podocytes, was increased significantly in the FSGS group. The ratio of two podocyte transcripts (either podocin:nephrin or desmin:nephrin), previously shown to be related to podocyte hypertrophic stress^{6,7}, were also increased in the TG.1K.ALD group that developed FSGS, but not in other groups. Rapamycin treatment itself markedly reduced podocyte transcript expression thereby making interpretation of transcriptomic data in the setting of rapamycin difficult. ACE inhibition may have had minor effects on transcript levels that were not significant in the ratio data. These data show that there were two different reasons for podocyte transcript changes, (a) podocyte density was decreased due to accumulation of non-podocyte glomerular cells, and (b) relative expression of podocyte genes was also altered compatible with podocytes undergoing hypertrophic stress in association with FSGS lesion development. Reduction in the podocyte transcriptomic signal was not due to preferential loss of podocytes from glomeruli. Abbreviations as follows: TG, Fischer344 transgenic rats; WT, wild type Fischer344 rats; 1K/2K, nephrectomized/sham-nephrectomized; ALD, adlib diet; CRD, 40% calorie reduced diet; rapa, rapamycin-treated; ACEi, treated with the angiotensin II inhibitor enalapril. Data are shown as the mean±1SD. Comparisons were performed by ANOVA using the Bonferroni correction. *= $P < 0.05$, **= $P < 0.01$. TG=transgenic rats, WT=wild type Fischer344 rats, 1K/2K=nephrectomized/sham-nephrectomized, ALD=adlib diet, CRD=40% calorie reduced diet, rapa=rapamycin-treated, ACEi=treated with angiotensin II inhibitor enalapril.

Table 5

Categories	Diseases or functions annotation	p-Value	Molecules	Molecules
1 Cell Cycle, Cellular Assembly and Organization, DNA replication, Recombination and Repair	Segregation of chromosomes	7.4E-25	ATRX,AURKB,BUB1,CCNA2,CCNB1,CCNB2,CDC14A,CENPE,CENPF,CENPT,ECT2,HJURP,HMMR,KIF11,KIF2C,KMT5B,KNSTRN,LATS1,LMNA,NCAPD2,NCAPD3,NCAPG,NDC80,NINL,NUF2,NUSAP1,PLK1,PTTG1,SGO1,STAG1,STAG2,TOP2A,TPX2,ZWINT	34
2 Cell Cycle	Arrest in mitosis	1.6E-17	AURKB,BUB1,BUB1B,CDC20,CDK1,CENPE,CENPI,CSNK1A1,DCTN2,KIF11,KIF4A,KNL1,KNTC1,MYBL2,NDC80,NUF2,PDLIM7,PLK1,PURA,RACGAP1,SGO1,TPX2,ZWINT	23
3 Cell Cycle	Mitosis	1.9E-17	AURKB,BCL2,BMP2,BUB1,BUB1B,CCNA2,CCNB1,CDC14A,CDC20,CDC25C,CDK1,CENPE,CENPF,CENPI,CENPT,CLASP2,CSNK1A1,DCTN2,DLGAP5,DYNLT3,FBXW5,FOXM1,GADD45B,JUN,KIF11,KIF18A,KIF18B,KIF2C,KIF4A,KNL1,KNTC1,LATS1,LATS2,MYBL2,NDC80,NINL,NRG1,NUF2,NUSAP1,PDGFRA,PDLIM7,PHB2,PHIP,PLK1,PTHLH,PTTG1,PURA,RACGAP1,SGO1,SLC9A3R1,SPP1,TNC,TOP2A,TPX2,TRIM33,YWHAE,ZWINT	57
4 Cell Cycle	M phase	1.1E-16	AURKB,BCL2,BUB1B,CCNB1,CD2AP,CDC14A,CDC20,CDK1,CENPE,DIAPH3,ECT2,GIPC1,HMMR,KIF14,KIF20A,KIF20B,KIF23,KIF4A,KLHL9,LATS1,LATS2,LMNA,mir-23,NCAPD2,NDC80,NUF2,NUSAP1,PFN1,PLK1,PRC1,PTTG1,RAB11FIP3,RACGAP1,RHOC,STAG1,TOP2A,TOPAZ1	37

Table 5 legend: Ingenuity Pathway Analysis of glomerular genes. 538 genes (shown in Supplemental Table 2) were expressed significantly differently (either up or down) between the TG.1K.ALD rats that developed FSGS and the three groups that were prevented by treatment from developing FSGS (TG.1K.CRD, TG.1K.Rapa and TG.1K.ACEi). Ingenuity Pathway analysis of these genes in the Diseases or functions annotation showed that the top 35 were designated either as cell cycle or various cancers. The top four candidates, all designated as different aspects of cell cycle, with overlapping genes are shown. Transcript levels for the 84 genes identified in Table 5 relative to the TG.1K.ALD group are shown in Supplementary Table 3.

Table 6

Reference	Comparison disease	P value	Q value	Gene #
Increasesers (n=376 genes)				
Ju	Lupus nephritis vs HLD	2.6E-40	3.3E-37	105
Ju	Diabetic neph vs HLD	2.0E-30	1.3E-27	92
Ju	Membranous neph vs HLD	3.1E-26	1.8E-23	86
Ju	Vasculitic neph vs HLD	3.1E-24	1.4E-21	83
Ju	IgA neph vs HLD	8.2E-16	2.7E-13	69
Ju	FSGS vs HLD	3.3E-14	7.8E-12	66
Decreasers (n=239 genes)				
Hodgin	Collapsing FSGS vs NLD	1.5E-8	1.5E-5	34
Hodgin	FSGS vs NLD	4.2E-6	0.002	46
Ju	IgA neph vs HLD	3.8E-7	2.4E-4	37
Ju	Lupus neph vs HLD	1.1E-6	6.2E-4	27
Ju	Diabetic neph vs HLD	2.3E-6	0.002	27

Table 6 legend. Comparison of the rat FSGS transcriptomic profile with human glomerular transcriptomic profiles derived from the Nephroseq database. There were 800 genes differently expressed (1.5-fold change $P < 0.05$) between glomeruli in which FSGS developed (TG.1K.ALD) versus the TG.1K.CRD) where FSGS did not occur. The TG.1K.ALD.Rapa and TG.1K.ALD.ACEi groups were not included because of potential drug effects on the gene expression profiles. Of these 800 rat genes 185 were not recognized by the Nephroseq database, leaving 615 genes for analysis of which 376 were significantly increased and 239 were significantly decreased in association with FSGS lesion formation. These two gene sets were then used to search the Nephroseq database for correlations to previously reported glomerular disease datasets for increasing and decreasing genes associated with glomerular diseases. Ju and

Hodgin refer to Nephroseq data ⁸. NLD and HLD refer to normal living donor as a source for comparison to pathologic glomeruli. Neph stands for nephropathy.

Title: FSGS as an adaptive response to growth-induced podocyte stress

Nishizono et al.

Supplemental Table 1

	n	Weight (g)	Δ weight (%)	Ucreatinine (mg/24hrs)	Ucreatinine (% change)	Uurea (mg/24hrs)	Uprotein (mg/24hrs)	UProtCR	GS (%)	Protection
Time of nephrectomy	49	297±3		9.4±1.0		527±47	13±1	1.5±0.2	0	
At end of 16 week study										
Regular diet	6	374±14	+26%	13.4±0.7	+43%	1,071±22	75±10	5.5±0.6	39±6	No
40% Calorie reduction	6	237±5	-20%	7.2±0.2	-24%	580±45	7±1	1.0±0.2	0	Yes
20% Calorie reduction	6	296±5	0%	7.9±0.6	-16%	495±15	11±1	1.4±0.2	0	Yes
High protein	8	368±15	+24%	11.6±0.9	+23%	1,574±115	61±7	5.7±0.6	38±8	No
Low protein	7	410±7	+38%	11.0±0.9	+11%	128±44	13±2	1.2±0.2	0	Yes
High fat	5	406±7	+37%	10.9±0.4	+16%	548±36	26±4	2.4±0.3	15±5	Partial
High fat + sucrose	6	405±9	+36%	12.6±1.1	+34%	664±34	75±4	6.1±0.4	32±9	No
Regular diet + sucrose	5	401±3	+35%	13.8±0.4	+47%	639±25	76±10	5.5±0.9	35±5	No

Supplemental Table 1. Legend: Effect of modulating diet on post-nephrectomy hypertrophic glomerular injury. To simulate hypertrophic events post implantation adult heterozygous AA-4E-BP1 transgenic rats were nephrectomized at 300g and then placed on various diets for 14 weeks to determine the extent to which post-nephrectomy dietary modulation could protect against hypertrophic stress-induced glomerular injury. Urine creatinine excretion per 24 hours is a measure of muscle mass. The change in 24hour urine creatinine is a measure of change in muscle mass on the diet. Urine urea excretion per 24 hours was used to assess protein intake and catabolism. Urine protein excretion per 24 hours was used to assess the glomerular protein leak. Glomerulosclerosis (GS) (% glomeruli with adhesions) was used to assess degree of glomerular injury. 40% calorie restriction provided kidney protection but was associated with weight loss and loss of muscle mass and a higher than expected urea excretion suggesting that these animals may have been catabolic. 20% calorie restriction also provided good protection and was not associated with weight loss although muscle mass did decrease 16% over 16 weeks. Low protein diet provided protection, allowed weight gain and did not reduce muscle mass over the 16week period of observation. High fat diet provided partial protection possibly because of associated moderately reduced protein and carbohydrate intake, but if carbohydrate was added as 10% sucrose to drinking water to simulate drinking commercially available beverages (sodas) containing sugar the protection was lost. Regular diet with 10% sucrose added to drinking water significantly reduced urine urea excretion demonstrating that animals preferred drinking sweetened water to eating regular food. High protein diet was not different from regular diet by any criterion measured. These data demonstrate how nephrectomy-induced hypertrophic events can be significantly impacted by modulating diet.

Supplemental Table 2

Symbol	TG.1K.CRD	TG.1K.Rapa	TG.1K.ACEi
<i>Aars</i>	-0.386	-0.253	-0.185
<i>Abcb1b</i>	-0.757	-0.802	-0.938
<i>Abcc2</i>	-0.831	-0.471	-0.506
<i>Abhd17c</i>	-0.474	-0.728	-0.431
<i>Ablim1</i>	-0.179	-0.14	-0.393
<i>Acox3</i>	-0.31	-0.204	-0.151
<i>Adam15</i>	-0.416	-0.336	-0.42
<i>Adap1</i>	-0.515	-0.912	-0.569
<i>Adh1</i>	-0.475	-1.468	-0.581
<i>Adrm1</i>	-0.22	-0.455	-0.179
<i>Agpat4</i>	0.191	0.195	0.323
<i>Agtrap</i>	-0.306	-0.237	-0.226
<i>Agxt2</i>	-0.507	-0.666	-0.57
<i>Ahcyl1</i>	0.097	0.135	0.115
<i>Aifm1</i>	-0.271	-0.21	-0.346
<i>Ak2</i>	-0.531	-0.79	-0.494
<i>Akap9</i>	0.223	0.187	0.223
<i>Akr1a1</i>	-0.494	-0.305	-0.296
<i>Aldh7a1</i>	-0.373	-0.501	-0.402
<i>Aldob</i>	-0.234	-0.314	-0.335
<i>Alkbh3</i>	-0.134	-0.417	-0.198
<i>Ankle1</i>	-0.515	-0.654	-0.746
<i>Ankrd44</i>	0.337	0.605	0.303
<i>Apcs</i>	-0.553	-1.447	-0.658
<i>Apeh</i>	-0.239	-0.171	-0.239
<i>Arap2</i>	0.451	0.68	0.453
<i>Arhgef18</i>	0.646	0.21	0.282
<i>Arhgef25</i>	-0.266	-0.525	-0.338
<i>Arhgef26</i>	0.371	0.362	0.444
<i>Arid4a</i>	0.378	0.709	0.506
<i>Aspm</i>	-1.376	-0.712	-0.598
<i>Atf7ip</i>	0.203	0.149	0.244
<i>Atg13</i>	0.248	0.54	0.209
<i>Atp11c</i>	0.25	0.548	0.293
<i>Atp5a1</i>	-0.22	-0.189	-0.309
<i>Atp6v0d1</i>	-0.201	-0.451	-0.209
<i>Atp6v1b2</i>	-0.378	-0.481	-0.361
<i>Atp6v1c1</i>	-0.205	-0.282	-0.217
<i>Atraid</i>	-0.286	-0.18	-0.299
<i>Atrx</i>	0.26	0.292	0.34
<i>Aurkb</i>	-1.121	-1.068	-0.563
<i>B3gat1</i>	-1.42	-2.803	-1.458
<i>Bcl2</i>	0.275	0.86	0.463

<i>Bdp1</i>	0.337	0.362	0.299
<i>Blzf1</i>	0.308	0.368	0.268
<i>Bmp2</i>	-0.631	-1.321	-0.574
<i>Boc</i>	0.389	0.482	0.506
<i>Bub1</i>	-1.395	-0.957	-0.699
<i>Bub1b</i>	-0.932	-0.808	-0.481
<i>C4b</i>	-1.408	-1.806	-1.287
<i>C7</i>	-1.259	-1.741	-0.854
<i>Cachd1</i>	0.315	0.474	0.262
<i>Cacnb2</i>	0.477	0.892	0.906
<i>Calml4</i>	-0.281	-0.437	-0.259
<i>Capg</i>	-0.943	-0.633	-0.877
<i>Car7</i>	-0.933	-0.619	-0.397
<i>Cb707485</i>	-0.569	-0.57	-0.742
<i>Cbs</i>	-0.437	-0.761	-0.431
<i>Ccbl1</i>	-0.425	-0.977	-0.56
<i>Ccdc102a</i>	-0.386	-0.326	-0.294
<i>Ccl2</i>	-0.548	-0.818	-0.656
<i>Ccna2</i>	-1.113	-0.728	-0.383
<i>Ccnb1</i>	-1.371	-1.055	-0.63
<i>Ccnb2</i>	-2.034	-1.715	-0.703
<i>Cd276</i>	-0.539	-0.543	-0.36
<i>Cd2ap</i>	0.529	0.307	0.285
<i>Cd63</i>	-0.349	-0.57	-0.308
<i>Cdc14a</i>	0.409	0.174	0.184
<i>Cdc20</i>	-1.649	-0.819	-0.907
<i>Cdc25c</i>	-0.53	-0.66	-0.477
<i>Cdc73</i>	0.264	0.161	0.193
<i>Cdk1</i>	-1.591	-0.679	-0.489
<i>Cdkn2c</i>	-1.204	-0.648	-0.742
<i>Cdkn3</i>	-1.684	-1.024	-0.78
<i>Cdsn</i>	-0.934	-1.674	-1.22
<i>Cenpe</i>	-1.267	-0.844	-0.514
<i>Cenpf</i>	-1.458	-1.047	-0.911
<i>Cenpi</i>	-0.4	-0.377	-0.304
<i>Cenpt</i>	-0.505	-0.599	-0.437
<i>Cep170b</i>	-0.202	-1.031	-0.334
<i>Cfi</i>	-1.034	-0.78	-0.694
<i>Cflar</i>	0.211	0.44	0.245
<i>Cib1</i>	-0.347	-0.418	-0.381
<i>Clasp2</i>	0.184	0.371	0.222
<i>Clec1a</i>	0.293	0.802	0.342
<i>Clmp</i>	-0.706	-0.633	-0.63
<i>Clta</i>	-0.114	-0.169	-0.17
<i>Cluh</i>	-0.236	-0.266	-0.308
<i>Cndp2</i>	-0.549	-0.403	-0.444

<i>Cnnm1</i>	-0.555	-0.713	-0.387
<i>Cnot4</i>	0.099	0.209	0.198
<i>Cntnap1</i>	-0.446	-1.359	-0.766
<i>Col16a1</i>	-0.346	-0.723	-0.358
<i>Col3a1</i>	-1.034	-1.613	-1.11
<i>Col5a1</i>	-0.515	-0.951	-0.255
<i>Col6a6</i>	-1.112	-1.859	-0.979
<i>Coq9</i>	-0.296	-0.373	-0.314
<i>Cox6a1</i>	-0.523	-0.392	-0.388
<i>Cpd</i>	0.286	0.267	0.266
<i>Cpne3</i>	0.121	0.347	0.174
<i>Cpne7</i>	-0.377	-1.786	-0.796
<i>Crebbp</i>	0.197	0.18	0.256
<i>Crip1</i>	-0.552	-0.54	-0.73
<i>Cript</i>	0.373	0.717	0.367
<i>Csnk1a1</i>	0.093	0.138	0.127
<i>Csrnp2</i>	0.36	0.466	0.348
<i>Ctsb</i>	-0.38	-0.52	-0.227
<i>Cxcr2</i>	0.563	1.449	1.193
<i>Cyp24a1</i>	-1.249	-1.823	-1.142
<i>Cytip</i>	0.421	0.929	0.815
<i>Dab2</i>	-0.163	-0.518	-0.298
<i>Dact2</i>	-0.363	-0.727	-0.898
<i>Dad1</i>	-0.453	-0.315	-0.249
<i>Dao</i>	-0.382	-0.796	-0.45
<i>Dap</i>	-0.27	-0.742	-0.301
<i>Dcn</i>	-1.277	-1.097	-1.096
<i>Dctn2</i>	-0.204	-0.182	-0.223
<i>Dcxr</i>	-0.331	-1.1	-0.771
<i>Ddx19a</i>	-0.373	-0.294	-0.441
<i>Decr2</i>	-0.465	-0.658	-0.354
<i>Depdc1</i>	-1.063	-0.743	-0.661
<i>Dera</i>	-0.352	-0.479	-0.18
<i>Dgcr8</i>	0.344	0.401	0.293
<i>Dhh</i>	-0.785	-0.593	-0.843
<i>Dhrs1</i>	-0.191	-0.508	-0.263
<i>Dhrs11</i>	-0.507	-0.441	-0.708
<i>Diaph3</i>	-1.622	-1.238	-0.741
<i>Dlc1</i>	0.315	0.456	0.441
<i>Dlgap5</i>	-1.472	-0.796	-0.681
<i>Dll1</i>	-0.308	-0.436	-0.47
<i>Dll4</i>	0.44	1.659	1.207
<i>Dmxl1</i>	0.159	0.167	0.186
<i>Dnajb4</i>	0.249	0.557	0.415
<i>Dnpep</i>	-0.296	-0.247	-0.236
<i>Dpep2</i>	-0.39	-1.165	-0.79

<i>Dph5</i>	-0.263	-0.292	-0.259
<i>Dph6</i>	0.254	0.767	0.257
<i>Dpp7</i>	-0.624	-1.794	-0.463
<i>Dpy19l4</i>	0.254	0.577	0.258
<i>Dpys</i>	-0.335	-0.769	-0.619
<i>Dynlt3</i>	0.174	0.276	0.17
<i>E2f7</i>	-0.682	-0.729	-0.516
<i>Eapp</i>	0.446	0.793	0.41
<i>Eci3</i>	-0.498	-0.514	-0.477
<i>Ecsit</i>	-0.29	-0.599	-0.215
<i>Ect2</i>	-1.604	-0.952	-0.59
<i>Efnb2</i>	0.257	0.89	0.632
<i>Eif3a</i>	0.123	0.13	0.139
<i>Elmo1</i>	-0.315	-0.348	-0.433
<i>Ero1a</i>	0.461	0.19	0.404
<i>Esf1</i>	0.302	0.312	0.271
<i>Etfb</i>	-0.259	-0.147	-0.237
<i>Exnef</i>	-0.356	-0.418	-0.411
<i>Ezh1</i>	0.14	0.391	0.18
<i>Ezh2</i>	-0.758	-0.517	-0.365
<i>Fabp4</i>	-1.193	-0.786	-1.247
<i>Fam111a</i>	-1.628	-1.055	-0.77
<i>Fam179b</i>	0.308	0.318	0.275
<i>Fam208a</i>	0.2	0.439	0.318
<i>Fam98a</i>	-0.113	-0.174	-0.17
<i>Fblim1</i>	-0.526	-0.894	-0.516
<i>Fbxw5</i>	-0.306	-0.334	-0.212
<i>Fga</i>	-1.187	-0.617	-1.222
<i>Fgfr4</i>	-0.418	-0.789	-0.689
<i>Fh</i>	-0.256	-0.187	-0.247
<i>Fndc5</i>	-0.418	-0.708	-0.488
<i>Foxj3</i>	0.295	0.297	0.344
<i>Foxm1</i>	-0.65	-0.884	-0.656
<i>Foxn3</i>	0.177	0.263	0.296
<i>Frs2</i>	0.231	0.426	0.336
<i>Ftl1</i>	-0.799	-0.665	-0.338
<i>Fxyd5</i>	-0.93	-0.629	-0.652
<i>Fyco1</i>	0.162	0.176	0.278
<i>Gabra1</i>	0.449	1.198	1.123
<i>Gadd45b</i>	0.32	0.334	0.295
<i>Gas2</i>	-0.64	-0.955	-0.476
<i>Gas2l3</i>	-1.72	-1.106	-0.494
<i>Gdf15</i>	-0.578	-1.219	-0.961
<i>Gipc1</i>	-0.657	-0.431	-0.345
<i>Gja1</i>	-0.437	-0.424	-0.494
<i>Glb1l</i>	-0.255	-0.533	-0.242

<i>Glb1l2</i>	-0.325	-0.553	-0.634
<i>Glis2</i>	-0.213	-0.4	-0.32
<i>Glrx5</i>	-0.379	-0.306	-0.381
<i>Gnaq</i>	0.195	0.505	0.33
<i>Gnat2</i>	-0.849	-1.749	-0.925
<i>Gne</i>	-0.279	-0.254	-0.23
<i>Gnpda1</i>	-0.547	-0.919	-0.402
<i>Gopc</i>	0.213	0.281	0.331
<i>Gosr2</i>	-0.151	-0.341	-0.215
<i>Got2</i>	-0.334	-0.361	-0.368
<i>Gppb1</i>	0.327	0.34	0.281
<i>Gpcpd1</i>	0.25	0.209	0.301
<i>Gpnmh</i>	-1.841	-1.117	-0.667
<i>Gpr146</i>	0.251	0.481	0.44
<i>Gprc5a</i>	-0.926	-1.184	-0.826
<i>Grk5</i>	0.338	0.288	0.26
<i>Gxylt1</i>	0.17	0.348	0.327
<i>H2afx</i>	-1.026	-0.743	-0.55
<i>Hao1</i>	-1.446	-1.589	-1.001
<i>Havcr1</i>	-4.047	-3.558	-3.712
<i>Hdac9</i>	-0.279	-0.242	-0.357
<i>Helz</i>	0.329	0.211	0.208
<i>Hgd</i>	-0.428	-0.662	-0.582
<i>Hipk3</i>	0.301	0.218	0.262
<i>Hist1h1a</i>	-0.717	-0.516	-0.471
<i>Hist1h2ah</i>	-1.559	-0.908	-0.463
<i>Hist1h2ai</i>	-1.553	-0.958	-0.805
<i>Hist1h2bcl1</i>	-0.841	-0.686	-0.586
<i>Hist1h2bf</i>	-1.259	-0.781	-0.803
<i>Hist1h2bk</i>	-0.554	-0.436	-0.422
<i>Hist1h3a</i>	-1.173	-0.837	-0.677
<i>Hist1h4a</i>	-0.928	-0.335	-0.371
<i>Hist2h4</i>	-1.567	-0.839	-0.996
<i>Hjurp</i>	-1.335	-0.952	-0.79
<i>Hmbox1</i>	0.254	0.529	0.388
<i>Hmgxb3</i>	-0.183	-0.245	-0.132
<i>Hmmr</i>	-1.556	-0.971	-0.848
<i>Hnf1a</i>	-0.403	-0.666	-0.621
<i>Homer3</i>	-0.22	-0.207	-0.185
<i>Hook2</i>	-0.51	-1.127	-0.628
<i>Hsd17b4</i>	-0.381	-0.272	-0.375
<i>Hspa14</i>	-0.252	-0.308	-0.178
<i>Hspg2</i>	-0.623	-0.895	-0.321
<i>Htra3</i>	-1.592	-0.799	-1.51
<i>Ifitm2</i>	-0.589	-0.258	-0.32
<i>Ift81</i>	0.217	0.255	0.126

<i>Il18rap</i>	0.675	1.07	1.033
<i>Iqgap3</i>	-1.609	-1.024	-0.658
<i>Jun</i>	0.25	0.575	0.125
<i>Kctd17</i>	-0.354	-0.806	-0.371
<i>Kdm4c</i>	0.153	0.16	0.145
<i>Kif11</i>	-0.854	-0.768	-0.584
<i>Kif12</i>	-0.385	-0.906	-0.816
<i>Kif14</i>	-0.772	-0.483	-0.478
<i>Kif18a</i>	-0.864	-0.551	-0.524
<i>Kif18b</i>	-1.166	-0.976	-0.608
<i>Kif1b</i>	0.145	0.088	0.232
<i>Kif20a</i>	-1.514	-1.055	-0.839
<i>Kif20b</i>	-1.001	-0.482	-0.494
<i>Kif23</i>	-1.161	-0.96	-0.52
<i>Kif2c</i>	-1.257	-1.019	-0.865
<i>Kif4a</i>	-1.348	-1.27	-0.564
<i>Kifc2</i>	-0.213	-0.397	-0.492
<i>Klhl9</i>	0.172	0.751	0.326
<i>Kmt2e</i>	0.223	0.335	0.248
<i>Kmt5b</i>	0.209	0.275	0.151
<i>Kn11</i>	-1.811	-0.974	-0.669
<i>Knstrn</i>	-1.221	-0.695	-0.555
<i>Kntc1</i>	-1.044	-0.706	-0.496
<i>Krt35</i>	0.769	0.833	0.365
<i>Lactb2</i>	-0.485	-0.347	-0.473
<i>Lamb1</i>	-0.416	-0.29	-0.616
<i>Lamb2</i>	0.133	0.155	0.271
<i>Lats1</i>	0.304	0.284	0.306
<i>Lats2</i>	0.435	0.184	0.334
<i>Lemd3</i>	0.287	0.389	0.28
<i>Lgals1</i>	-0.658	-1.012	-0.408
<i>Lgals3</i>	-1.701	-0.881	-0.529
<i>Lif</i>	-0.506	-1.013	-0.629
<i>Lifr</i>	0.382	0.943	0.572
<i>Lima1</i>	0.224	0.268	0.284
<i>Lmna</i>	-0.438	-0.486	-0.349
<i>LOC100359668</i>	-0.449	-0.959	-0.453
<i>LOC100360087</i>	-0.807	-0.737	-0.456
<i>LOC100362606</i>	-0.424	-0.54	-0.303
<i>LOC100363177</i>	-0.813	-1.085	-0.445
<i>LOC100364016</i>	-1.723	-1.031	-0.548
<i>LOC100912338</i>	-0.528	-0.312	-0.57
<i>LOC102551340</i>	0.559	1.22	0.545
<i>LOC102555086</i>	-0.359	-0.623	-0.248
<i>LOC102555377</i>	0.422	0.404	0.488
<i>LOC680498</i>	-0.74	-0.654	-0.462

<i>LOC684841</i>	-1.103	-0.835	-0.461
<i>LOC688389</i>	-0.458	-0.89	-0.507
<i>LOC688553</i>	-1.006	-1.163	-0.891
<i>LOC691135</i>	0.497	0.476	0.678
<i>Lpcat1</i>	0.31	0.515	0.351
<i>Lrch3</i>	0.291	0.197	0.252
<i>Lrrc16a</i>	-0.265	-0.756	-0.356
<i>Lrrn1</i>	0.377	1.224	1.342
<i>Luzp1</i>	0.392	0.312	0.324
<i>Lysmd3</i>	0.299	0.327	0.366
<i>Lyst</i>	0.191	0.362	0.253
<i>Mab21l3</i>	-0.487	-1.462	-0.947
<i>Mafk</i>	0.284	0.261	0.259
<i>Magi1</i>	0.249	0.245	0.195
<i>Man1a1</i>	0.522	0.283	0.318
<i>Mcm10</i>	-0.96	-0.693	-0.319
<i>Mcoln1</i>	-0.298	-0.197	-0.177
<i>Med13</i>	0.113	0.28	0.21
<i>Meis2</i>	0.142	0.519	0.217
<i>Melk</i>	-1.089	-0.774	-0.654
<i>Mettl10</i>	0.224	0.255	0.201
<i>Mettl14</i>	0.179	0.266	0.238
<i>Mgp</i>	-0.384	-0.376	-0.232
<i>Mir23a</i>	-0.742	-1.621	-0.954
<i>Mlph</i>	-0.772	-1.334	-0.58
<i>Mmp28</i>	-0.873	-0.69	-0.403
<i>Mmp8</i>	0.693	0.977	1.092
<i>Mns1</i>	-0.348	-0.438	-0.428
<i>Mob3b</i>	-0.482	-0.56	-0.635
<i>Mroh1</i>	-0.242	-0.52	-0.403
<i>Mrpl37</i>	-0.306	-0.609	-0.289
<i>Msl2</i>	0.218	0.334	0.27
<i>Mt1m</i>	-1.382	-1.165	-0.754
<i>Mterf1</i>	0.181	0.311	0.094
<i>Mtf2</i>	0.262	0.573	0.268
<i>Mtmr11</i>	-0.285	-0.528	-0.545
<i>Mxra8</i>	-0.407	-0.709	-0.27
<i>Myadm</i>	-0.45	-0.507	-0.239
<i>Mybl2</i>	-0.624	-0.446	-0.577
<i>Mybpc2</i>	-0.58	-1.093	-0.639
<i>Myo9a</i>	0.305	0.176	0.221
<i>Nabp1</i>	-0.375	-1.069	-0.623
<i>Nagk</i>	-0.304	-0.528	-0.394
<i>Naprt</i>	-0.42	-0.398	-0.407
<i>Nasp</i>	-0.413	-0.503	-0.345
<i>Ncapd2</i>	-0.532	-0.695	-0.546

<i>Ncapd3</i>	-0.279	-0.447	-0.203
<i>Ncapg</i>	-1.492	-1.293	-0.751
<i>Ncaph</i>	-1.679	-1.481	-0.858
<i>Ndc80</i>	-1.513	-0.751	-0.591
<i>Ndrp1</i>	-0.798	-0.594	-0.532
<i>Ndufa3</i>	-0.38	-0.467	-0.546
<i>Nefm</i>	-0.597	-1.429	-0.675
<i>Neil1</i>	-0.49	-0.603	-0.418
<i>Ninl</i>	-0.766	-1.41	-0.664
<i>Nipbl</i>	0.279	0.314	0.299
<i>Nit1</i>	-0.243	-0.334	-0.25
<i>Nmnat3</i>	-0.39	-0.505	-0.6
<i>Notch1</i>	0.273	0.688	0.534
<i>Npdc1</i>	-0.393	-0.569	-0.245
<i>Nr1h3</i>	-0.484	-0.687	-0.234
<i>Nrg1</i>	-0.687	-0.965	-0.695
<i>Nt5dc2</i>	-0.557	-0.806	-0.315
<i>Ntn4</i>	0.581	1.327	1.052
<i>Nubp2</i>	-0.353	-0.313	-0.278
<i>Nuf2</i>	-1.425	-0.961	-0.591
<i>Nusap1</i>	-1.393	-0.797	-0.622
<i>Opcml</i>	0.885	0.646	0.771
<i>Ophn1</i>	0.36	0.904	0.428
<i>Orc3</i>	0.136	0.339	0.149
<i>Otud4</i>	0.156	0.361	0.225
<i>Oxct1</i>	-0.335	-0.375	-0.453
<i>P2ry10</i>	0.293	0.862	0.645
<i>P2ry2</i>	-0.609	-0.902	-0.776
<i>Palm</i>	-0.409	-0.391	-0.365
<i>Parp3</i>	-0.355	-0.354	-0.291
<i>Pbx1</i>	0.346	0.514	0.473
<i>Pcmt1</i>	0.348	0.316	0.165
<i>PCOLCE2</i>	-0.802	-0.993	-0.864
<i>Pdcd4</i>	0.315	0.67	0.299
<i>Pdgfra</i>	-0.536	-0.804	-0.368
<i>Pdia5</i>	0.425	0.521	0.704
<i>Pdlim7</i>	-0.623	-1.088	-0.487
<i>Pdpr1</i>	0.152	0.356	0.184
<i>Pdzd2</i>	0.259	0.493	0.344
<i>Pecr</i>	-0.494	-0.49	-0.734
<i>Pex16</i>	-0.421	-0.343	-0.367
<i>Pfn1</i>	-0.319	-0.359	-0.211
<i>Phb2</i>	-0.336	-0.194	-0.247
<i>Phf3</i>	0.171	0.171	0.171
<i>Phip</i>	0.318	0.578	0.391
<i>Pi16</i>	-0.464	-0.8	-0.609

<i>Pias2</i>	0.238	0.412	0.242
<i>Pla2g16</i>	0.265	0.342	0.236
<i>Plcxd2</i>	-0.636	-0.824	-0.631
<i>Plekha3</i>	0.135	0.231	0.173
<i>Plekhb2</i>	-0.275	-0.252	-0.217
<i>Plk1</i>	-1.599	-1.077	-0.61
<i>Plp2</i>	-0.6	-0.439	-0.269
<i>Pls1</i>	-0.537	-0.566	-0.575
<i>Plxna4</i>	0.28	0.594	0.514
<i>Pnlcd1</i>	-0.384	-0.523	-0.467
<i>Pnpla8</i>	0.3	0.361	0.259
<i>Ppa2</i>	-0.37	-0.207	-0.306
<i>Ppef2</i>	-0.633	-0.527	-0.94
<i>Ppil4</i>	0.216	0.366	0.334
<i>Ppm1j</i>	-0.373	-0.86	-0.443
<i>Ppp4r1</i>	-0.229	-0.16	-0.136
<i>Ppp4r2</i>	0.252	0.377	0.209
<i>Ppp4r3b</i>	0.155	0.389	0.138
<i>Pqlc3</i>	-0.668	-0.508	-0.564
<i>Prc1</i>	-1.829	-1.279	-0.561
<i>Prex2</i>	0.285	0.66	0.737
<i>Prf1</i>	0.931	0.802	1.792
<i>Prkab1</i>	-0.268	-0.375	-0.283
<i>Prkar2a</i>	0.238	0.314	0.219
<i>Proser2</i>	0.48	0.641	0.53
<i>Prpf18</i>	0.185	0.229	0.183
<i>Prr11</i>	-0.921	-0.912	-0.471
<i>Prrc2c</i>	0.494	0.191	0.229
<i>Psph</i>	-0.333	-0.752	-0.321
<i>Ptbp3</i>	0.236	0.323	0.25
<i>Pthlh</i>	-0.541	-1.115	-0.603
<i>Ptpru</i>	0.522	0.454	0.49
<i>Ptprz1</i>	1.341	1.1	1.3
<i>Pttg1</i>	-1.013	-0.966	-0.591
<i>Pura</i>	0.251	0.424	0.337
<i>Pxk</i>	0.273	0.222	0.235
<i>Qdpr</i>	-0.374	-0.302	-0.438
<i>Qser1</i>	0.359	0.309	0.334
<i>Rab11fip3</i>	-0.276	-0.754	-0.34
<i>Racgap1</i>	-1.393	-0.952	-0.591
<i>Rai14</i>	0.189	0.367	0.234
<i>Rbms2</i>	0.334	0.375	0.324
<i>Rc3h1</i>	0.309	0.287	0.288
<i>Renbp</i>	-0.384	-1.45	-0.36
<i>RGD1306148</i>	0.197	0.204	0.139
<i>RGD1309534</i>	-0.288	-0.429	-0.395

<i>RGD1309730</i>	0.279	0.304	0.216
<i>RGD1562378</i>	-0.373	-0.236	-0.301
<i>RGD1562451</i>	-0.644	-0.715	-0.652
<i>RGD1562608</i>	0.37	0.208	0.303
<i>Rgs16</i>	-1.174	-0.704	-1.241
<i>Rgs6</i>	0.588	0.73	0.544
<i>Rhoc</i>	-0.44	-0.427	-0.316
<i>Rhod</i>	-0.411	-0.532	-0.387
<i>Rnase6</i>	0.502	0.732	1.314
<i>Rpp25</i>	-0.749	-1.202	-0.807
<i>Rprd2</i>	0.18	0.207	0.18
<i>Rrm2</i>	-1.503	-1.304	-0.769
<i>Rsf1</i>	0.179	0.402	0.236
<i>Samd15</i>	0.46	0.658	0.61
<i>Sat2</i>	-0.225	-0.646	-0.668
<i>Sbno2</i>	-0.375	-0.574	-0.203
<i>Scai</i>	0.37	0.29	0.249
<i>Scarf2</i>	-0.56	-0.569	-0.284
<i>Scly</i>	-0.562	-1.22	-0.657
<i>Sec63</i>	0.244	0.28	0.223
<i>Sell</i>	0.681	1.44	1.502
<i>Serinc2</i>	-0.673	-0.639	-0.503
<i>Serpinb8</i>	-0.447	-0.618	-0.561
<i>Serpine1</i>	-1.058	-1.035	-0.931
<i>Serpine2</i>	-0.632	-0.913	-0.441
<i>Serpinf2</i>	-0.53	-0.322	-0.497
<i>Sgo1</i>	-0.787	-0.715	-0.171
<i>Sidt2</i>	-0.224	-0.166	-0.202
<i>Slc12a8</i>	-0.318	-0.437	-0.358
<i>Slc1a5</i>	-0.477	-0.36	-0.425
<i>Slc22a12</i>	-0.409	-0.801	-0.537
<i>Slc25a37</i>	0.431	0.285	0.262
<i>Slc2a6</i>	-0.624	-0.555	-0.399
<i>Slc34a2</i>	-0.894	-1.281	-1.187
<i>Slc38a3</i>	-0.764	-0.687	-0.705
<i>Slc41a2</i>	-0.388	-0.878	-0.386
<i>Slc9a3r1</i>	-0.434	-0.498	-0.419
<i>Slc9a4</i>	-0.628	-0.419	-0.495
<i>Slmap</i>	0.331	0.456	0.277
<i>Smg7</i>	0.279	0.431	0.321
<i>Smim14</i>	0.19	0.461	0.307
<i>Snap91</i>	-0.404	-0.719	-0.397
<i>Snrpa</i>	-0.206	-0.316	-0.321
<i>Sos1</i>	0.384	0.28	0.323
<i>Sp4</i>	0.319	0.537	0.257
<i>Spata13</i>	0.507	0.429	0.466

<i>Spcs2</i>	0.186	0.71	0.26
<i>Spp1</i>	-1.367	-1.675	-1.645
<i>Srcin1</i>	-0.349	-1.042	-0.571
<i>Srebf1</i>	-0.538	-0.547	-0.605
<i>Stag1</i>	0.121	0.273	0.215
<i>Stag2</i>	0.123	0.351	0.197
<i>Stk38l</i>	-0.3	-0.432	-0.506
<i>Ston2</i>	0.316	0.416	0.275
<i>Stx8</i>	-0.543	-0.741	-0.475
<i>Tagln</i>	-1.537	-1.993	-0.57
<i>Taok1</i>	0.181	0.132	0.203
<i>Tbc1d1</i>	-0.552	-0.774	-0.432
<i>Tbc1d13</i>	-0.271	-0.372	-0.251
<i>Tbx10</i>	-0.472	-1.547	-0.697
<i>Tcea3</i>	-0.411	-0.611	-0.69
<i>Tceal9</i>	-0.265	-0.233	-0.231
<i>Tes</i>	-0.654	-0.389	-0.506
<i>Tff3</i>	-0.726	-1.021	-0.808
<i>Tgfbr3</i>	0.574	0.431	0.419
<i>Tgm2</i>	-0.437	-0.343	-0.212
<i>Tgoln2</i>	0.141	0.265	0.169
<i>Tmed8</i>	0.263	0.458	0.414
<i>Tmem150a</i>	-0.204	-0.46	-0.29
<i>Tmem183a</i>	-0.3	-0.279	-0.205
<i>Tmem37</i>	-0.528	-1.054	-0.446
<i>Tmem47</i>	0.286	0.992	0.496
<i>Tmem63b</i>	-0.136	-0.348	-0.136
<i>Tmppe</i>	0.283	0.483	0.445
<i>Tmtc1</i>	0.363	0.207	0.391
<i>Tnc</i>	-1.169	-1.224	-1.041
<i>Tnfsf10</i>	0.509	1.242	0.855
<i>Top2a</i>	-1.846	-0.908	-0.436
<i>Topaz1</i>	-0.715	-0.806	-0.799
<i>Tpx2</i>	-1.706	-1.075	-0.693
<i>Trappc1</i>	-0.469	-0.513	-0.373
<i>Trem2</i>	-0.874	-0.782	-0.549
<i>Trib2</i>	0.22	0.511	0.208
<i>Trim33</i>	0.278	0.229	0.216
<i>Trip11</i>	0.206	0.438	0.298
<i>Troap</i>	-1.571	-1.256	-0.81
<i>Ttc17</i>	0.186	0.399	0.285
<i>Tubb6</i>	-1.435	-0.412	-0.62
<i>Tusc3</i>	0.201	0.247	0.128
<i>Uap1l1</i>	-0.454	-1.125	-0.409
<i>Ube2t</i>	-0.744	-0.508	-0.477
<i>Ubqln4</i>	-0.251	-0.147	-0.249

<i>Ufl1</i>	0.178	0.35	0.205
<i>Ugcg</i>	0.745	0.587	0.5
<i>Ugdh</i>	-0.42	-0.325	-0.267
<i>Uhrf1</i>	-1.345	-0.67	-0.444
<i>Unc5c</i>	0.641	0.677	0.511
<i>Uqcrc1</i>	-0.285	-0.232	-0.268
<i>Usp25</i>	0.196	0.315	0.205
<i>Usp48</i>	0.148	0.21	0.256
<i>Vim</i>	-0.192	-0.485	-0.274
<i>Vps13a</i>	0.33	0.183	0.214
<i>Vps29</i>	-0.237	-0.441	-0.276
<i>Wdr44</i>	0.294	0.279	0.269
<i>Wdr72</i>	-0.365	-0.307	-0.432
<i>Wnk4</i>	-0.449	-1.105	-0.869
<i>Wwc3</i>	0.253	0.251	0.251
<i>Xpnpep1</i>	-0.203	-0.366	-0.289
<i>Xylb</i>	-0.404	-0.908	-0.573
<i>Ypel2</i>	-0.561	-0.299	-0.424
<i>Ywhae</i>	-0.114	-0.097	-0.073
<i>Zbtb10</i>	0.623	0.297	0.322
<i>Zbtb11</i>	0.257	0.358	0.238
<i>Zcchc11</i>	0.304	0.281	0.21
<i>Zcchc6</i>	0.199	0.31	0.33
<i>Zdhhc17</i>	0.147	0.438	0.172
<i>Zeb1</i>	0.217	0.167	0.249
<i>Zfp280c</i>	0.187	0.233	0.239
<i>Zfp280d</i>	0.356	0.229	0.232
<i>Zfp292</i>	0.363	0.498	0.251
<i>Zfp354c</i>	0.556	0.769	0.829
<i>Zfp62</i>	0.187	0.372	0.203
<i>Zfp638</i>	0.252	0.362	0.252
<i>Zfp1</i>	-0.2	-0.346	-0.181
<i>Zhx1</i>	0.23	0.318	0.255
<i>Zmynd11</i>	0.273	0.273	0.153
<i>Zwint</i>	-0.27	-0.341	-0.378

Supplemental Table 2 legend: Log Fold changes(\log_2) for 538 genes expressed significantly differently (either up or down) between the TG.1K.ALD rats that developed FSGS and the three groups that were prevented by treatment from developing FSGS (TG.1K.CRD, TG.1K.Rapa and TG.1K.ACEi).

Supplemental Table 3

GeneSymbol	log ₂ fc_CR.Adlib	log ₂ fc_Rapa.Adlib	log ₂ fc_ACE.Adlib	Categories in Table5
<i>Aurkb</i>	-1.12	-1.07	-0.56	1,2,3,4
<i>Cenpe</i>	-1.27	-0.84	-0.51	1,2,3,4
<i>Ndc80</i>	-1.51	-0.75	-0.59	1,2,3,4
<i>Nuf2</i>	-1.42	-0.96	-0.59	1,2,3,4
<i>Plk1</i>	-1.60	-1.08	-0.61	1,2,3,4
<i>Bub1</i>	-1.39	-0.96	-0.70	1,2,3
<i>Kif11</i>	-0.85	-0.77	-0.58	1,2,3
<i>Sgo1</i>	-0.79	-0.71	-0.17	1,2,3
<i>Tpx2</i>	-1.71	-1.07	-0.69	1,2,3
<i>Zwint</i>	-0.27	-0.34	-0.38	1,2,3
<i>Bub1b</i>	-0.93	-0.81	-0.48	2,3,4
<i>Cdc20</i>	-1.65	-0.82	-0.91	2,3,4
<i>Cdk1</i>	-1.59	-0.68	-0.49	2,3,4
<i>Kif4a</i>	-1.35	-1.27	-0.56	2,3,4
<i>Racgap1</i>	-1.39	-0.95	-0.59	2,3,4
<i>Ccnb1</i>	-1.37	-1.06	-0.63	1,3,4
<i>Cdc14a</i>	0.41	0.17	0.18	1,3,4
<i>Lats1</i>	0.30	0.28	0.31	1,3,4
<i>Nusap1</i>	-1.39	-0.80	-0.62	1,3,4
<i>Pttg1</i>	-1.01	-0.97	-0.59	1,3,4
<i>Top2a</i>	-1.85	-0.91	-0.44	1,3,4
<i>Cenpi</i>	-0.40	-0.38	-0.30	2,3
<i>Csnk1a1</i>	0.09	0.14	0.13	2,3
<i>Dctn2</i>	-0.20	-0.18	-0.22	2,3
<i>Kn11</i>	-1.81	-0.97	-0.67	2,3
<i>Kntc1</i>	-1.04	-0.71	-0.50	2,3
<i>Mybl2</i>	-0.62	-0.45	-0.58	2,3
<i>Pdlim7</i>	-0.62	-1.09	-0.49	2,3
<i>Pura</i>	0.25	0.42	0.34	2,3
<i>Ccna2</i>	-1.11	-0.73	-0.38	1,3
<i>Cenpf</i>	-1.46	-1.05	-0.91	1,3
<i>Cenpt</i>	-0.51	-0.60	-0.44	1,3
<i>Kif2c</i>	-1.26	-1.02	-0.87	1,3
<i>Ninl</i>	-0.77	-1.41	-0.66	1,3
<i>Bcl2</i>	0.28	0.86	0.46	3,4
<i>Lats2</i>	0.44	0.18	0.33	3,4

<i>Ect2</i>	-1.60	-0.95	-0.59	1,4
<i>Hmnr</i>	-1.56	-0.97	-0.85	1,4
<i>Lmna</i>	-0.44	-0.49	-0.35	1,4
<i>Ncapd2</i>	-0.53	-0.70	-0.55	1,4
<i>Stag1</i>	0.12	0.27	0.21	1,4
<i>Cd2ap</i>	0.53	0.31	0.29	4
<i>Diaph3</i>	-1.62	-1.24	-0.74	4
<i>Gipc1</i>	-0.66	-0.43	-0.34	4
<i>Kif14</i>	-0.77	-0.48	-0.48	4
<i>Kif20a</i>	-1.51	-1.05	-0.84	4
<i>Kif20b</i>	-1.00	-0.48	-0.49	4
<i>Kif23</i>	-1.16	-0.96	-0.52	4
<i>Klhl9</i>	0.17	0.75	0.33	4
<i>mir-23</i>	-0.74	-1.62	-0.95	4
<i>Pfn1</i>	-0.32	-0.36	-0.21	4
<i>Prc1</i>	-1.83	-1.28	-0.56	4
<i>Rab11fip3</i>	-0.28	-0.75	-0.34	4
<i>Rhoc</i>	-0.44	-0.43	-0.32	4
<i>Topaz1</i>	-0.71	-0.81	-0.80	4
<i>Bmp2</i>	-0.63	-1.32	-0.57	3
<i>Cdc25c</i>	-0.53	-0.66	-0.48	3
<i>Clasp2</i>	0.18	0.37	0.22	3
<i>Dlgap5</i>	-1.47	-0.80	-0.68	3
<i>Dynlt3</i>	0.17	0.28	0.17	3
<i>Fbxw5</i>	-0.31	-0.33	-0.21	3
<i>Foxm1</i>	-0.65	-0.88	-0.66	3
<i>Gadd45b</i>	0.32	0.33	0.30	3
<i>Jun</i>	0.25	0.58	0.13	3
<i>Kif18a</i>	-0.86	-0.55	-0.52	3
<i>Kif18b</i>	-1.17	-0.98	-0.61	3
<i>Nrg1</i>	-0.69	-0.96	-0.70	3
<i>Pdgfra</i>	-0.54	-0.80	-0.37	3
<i>Phb2</i>	-0.34	-0.19	-0.25	3
<i>Phip</i>	0.32	0.58	0.39	3
<i>Pthlh</i>	-0.54	-1.12	-0.60	3
<i>Slc9a3r1</i>	-0.43	-0.50	-0.42	3
<i>Spp1</i>	-1.37	-1.68	-1.65	3
<i>Tnc</i>	-1.17	-1.22	-1.04	3
<i>Trim33</i>	0.28	0.23	0.22	3
<i>Ywhae</i>	-0.11	-0.10	-0.07	3
<i>Atrx</i>	0.26	0.29	0.34	1

<i>Ccnb2</i>	-2.03	-1.72	-0.70	1
<i>Hjurp</i>	-1.33	-0.95	-0.79	1
<i>Kmt5b</i>	0.21	0.27	0.15	1
<i>Knstrn</i>	-1.22	-0.70	-0.56	1
<i>Ncapd3</i>	-0.28	-0.45	-0.20	1
<i>Ncapg</i>	-1.49	-1.29	-0.75	1
<i>Stag2</i>	0.12	0.35	0.20	1

Supplemental Table 3 legend: Subset of the 538 genes shown in Supplemental Table 2 as identified in Table 5 by Ingenuity Pathway Analysis as related to cell cycling.

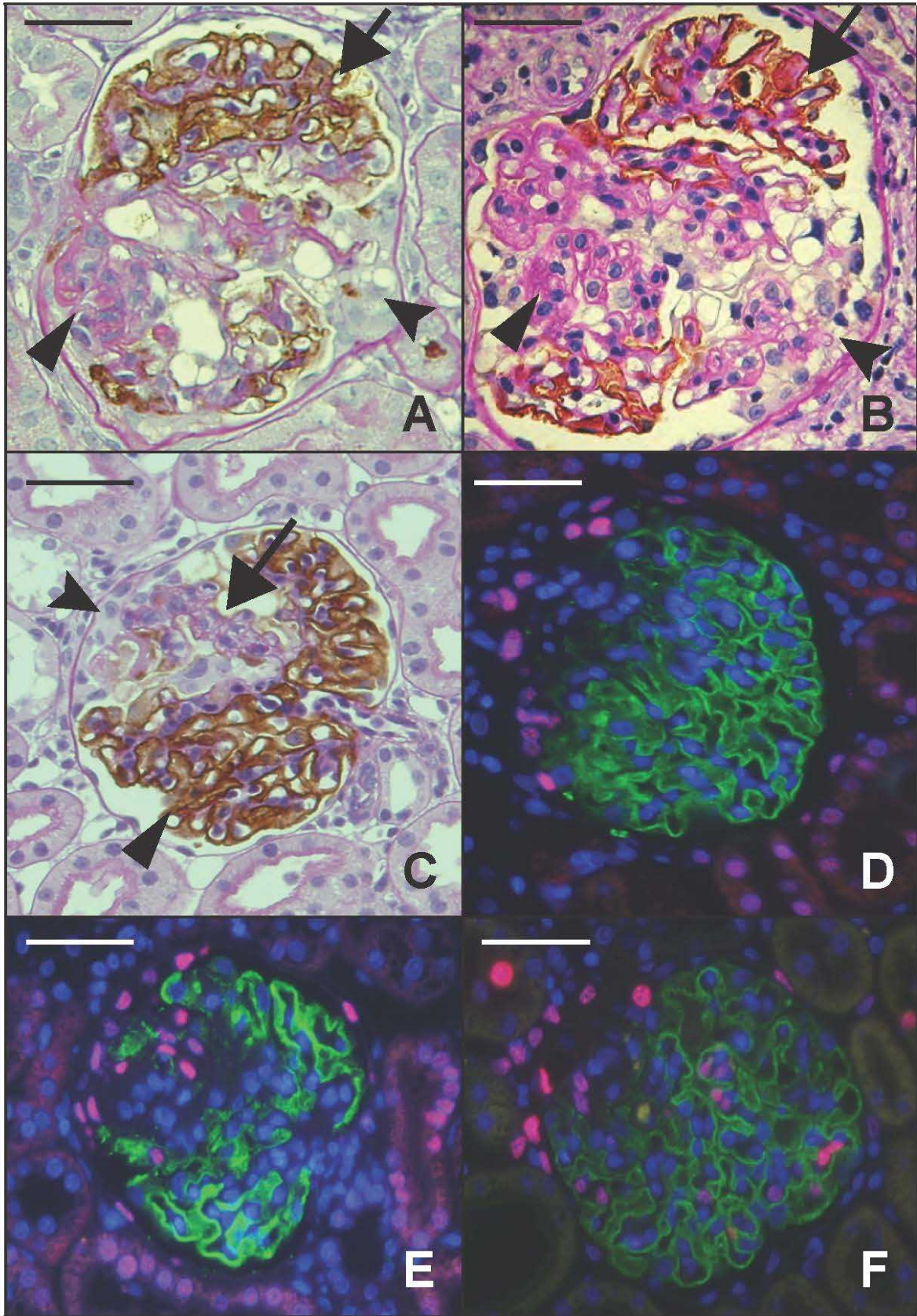


Figure. 1

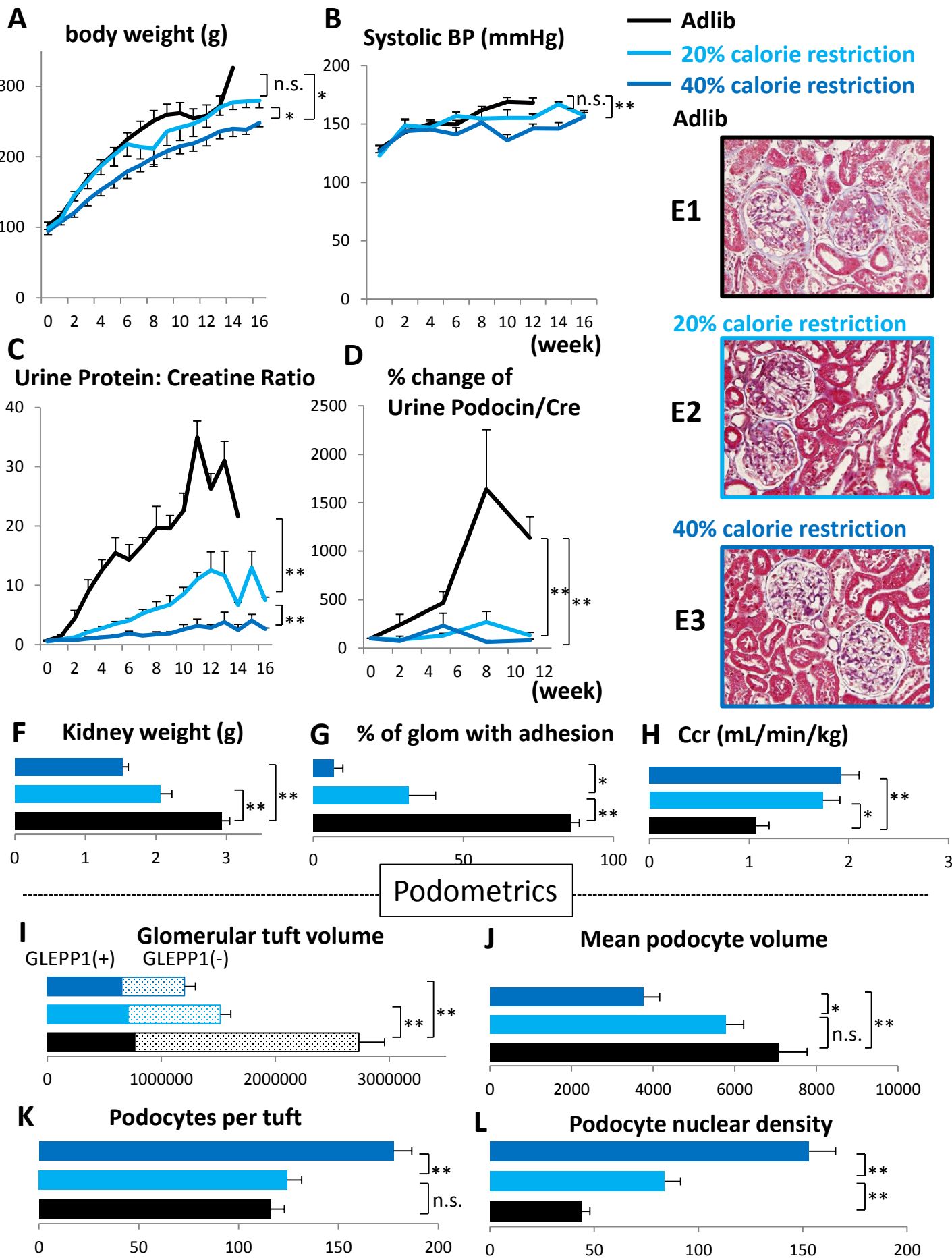


Figure. 2

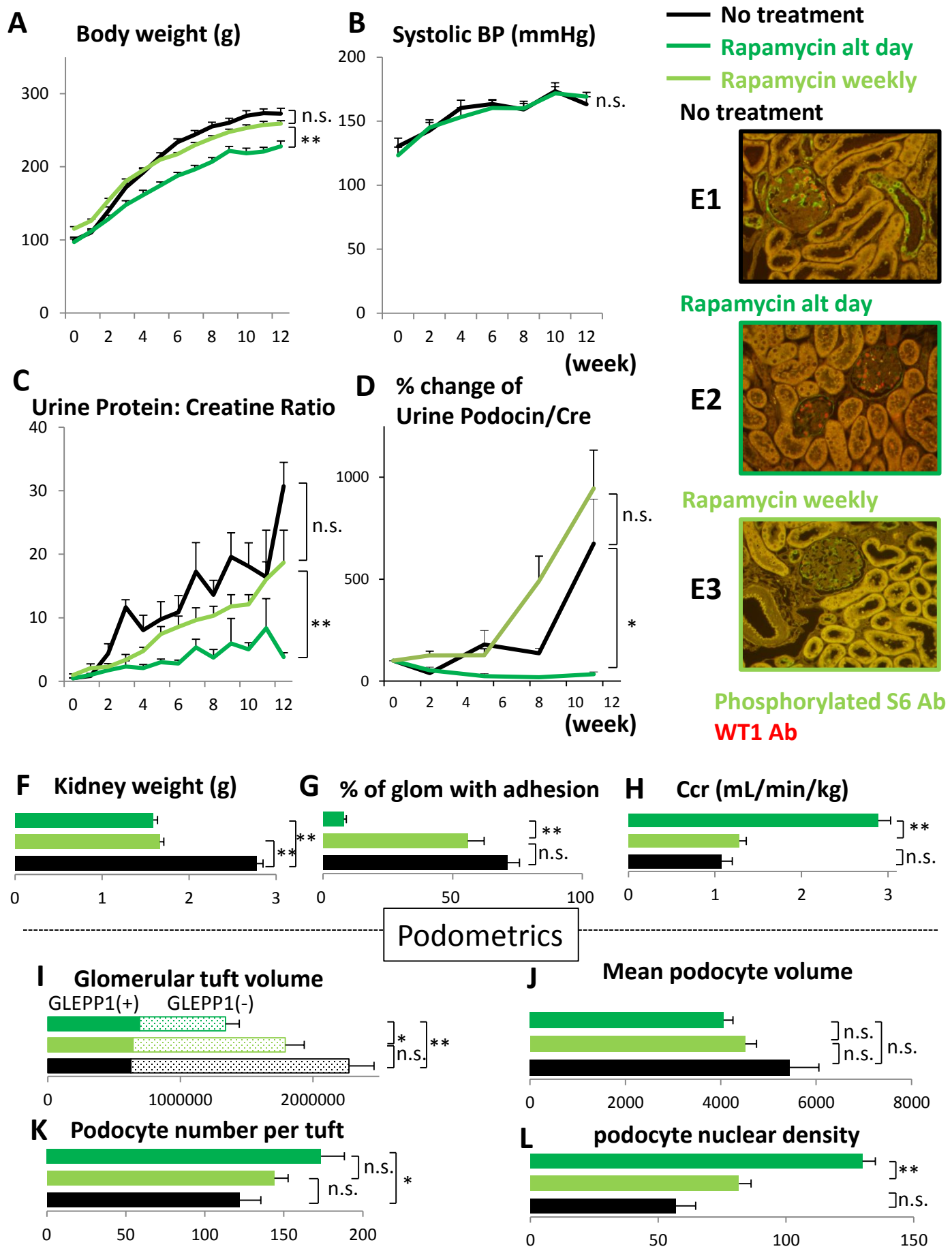


Figure. 3

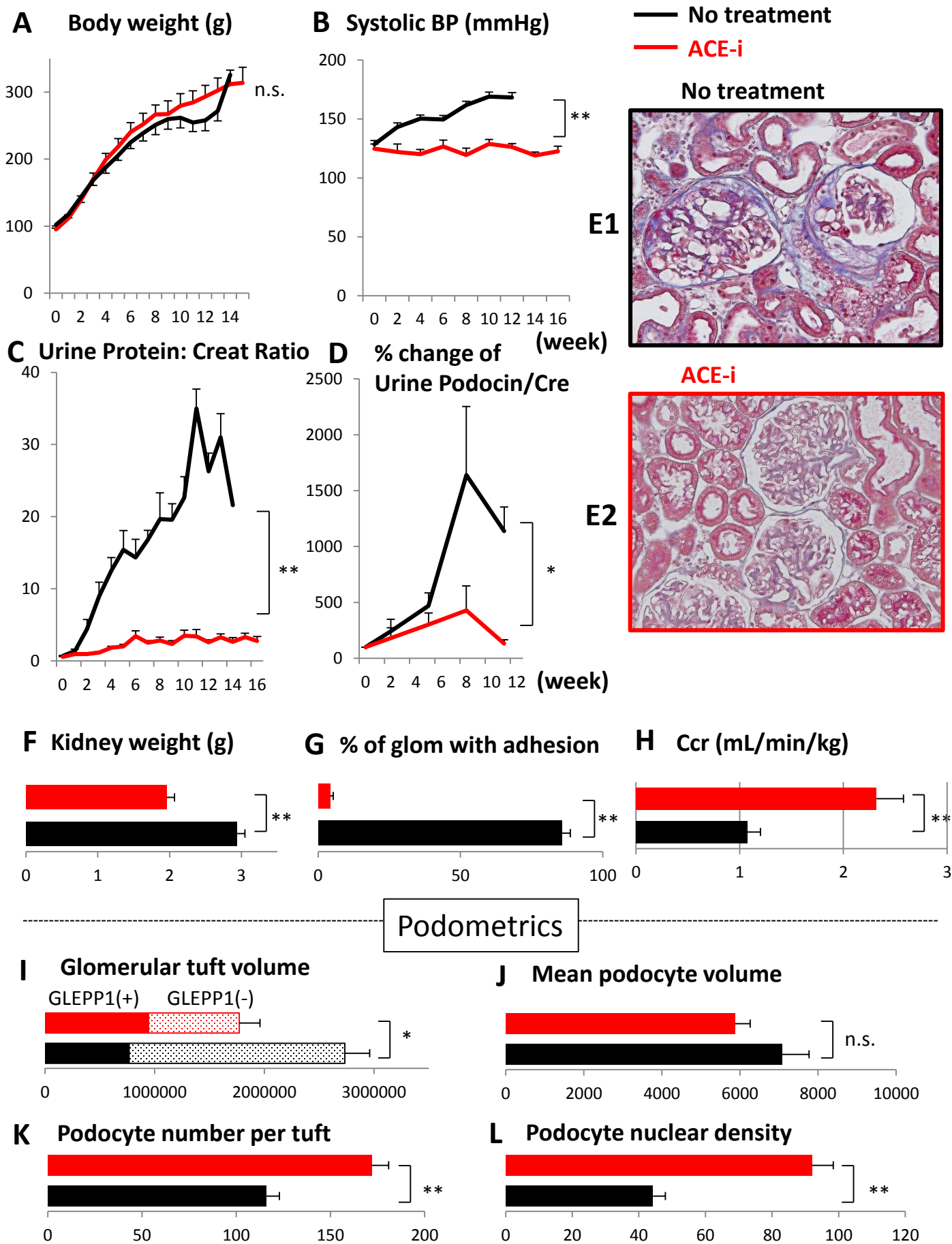


Figure. 4

— Early intervention at day +1

--- Late intervention at day +21

Rapamycin

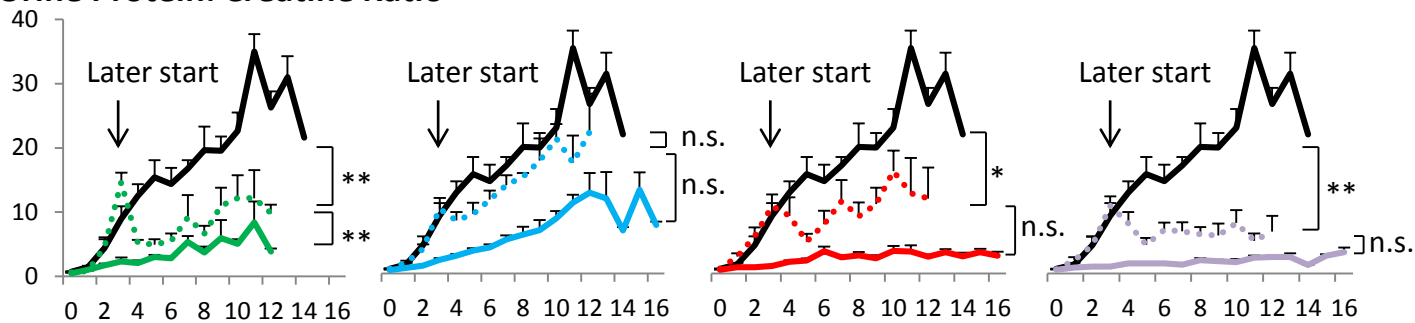
20%CR

ACE-i

20%CR + ACE-i

A

Urine Protein: Creatine Ratio



B

Kidney weight (g)



C

% of glomerulus with adhesion

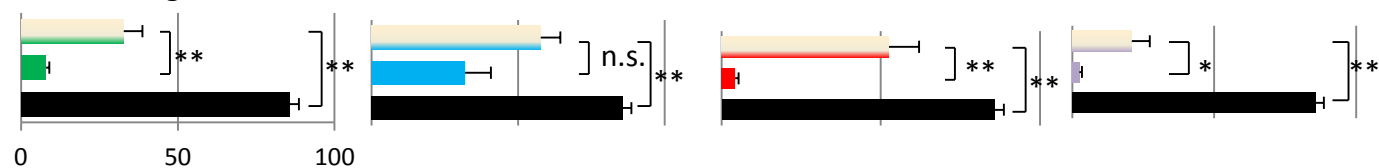


Figure. 5

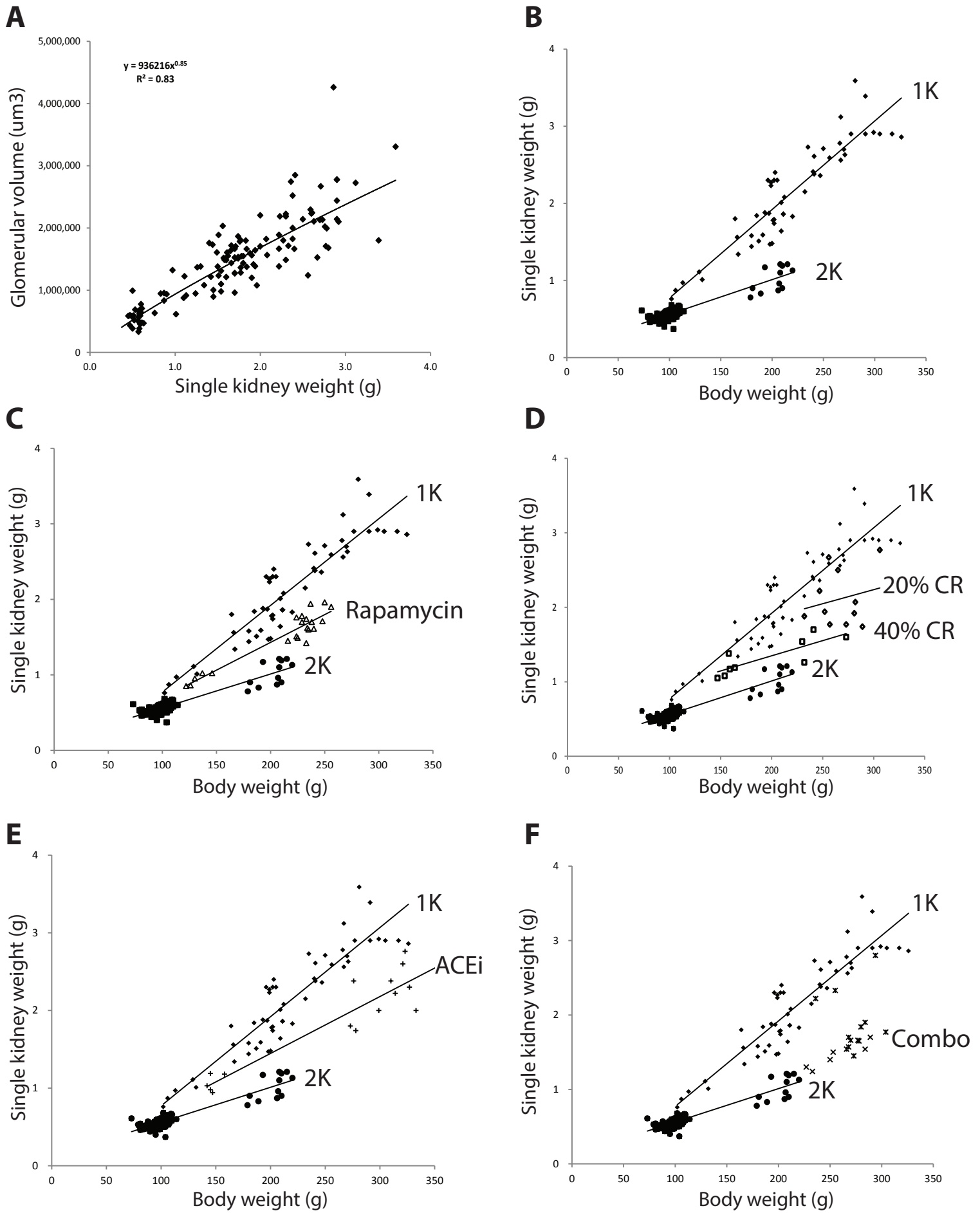


Figure. 6

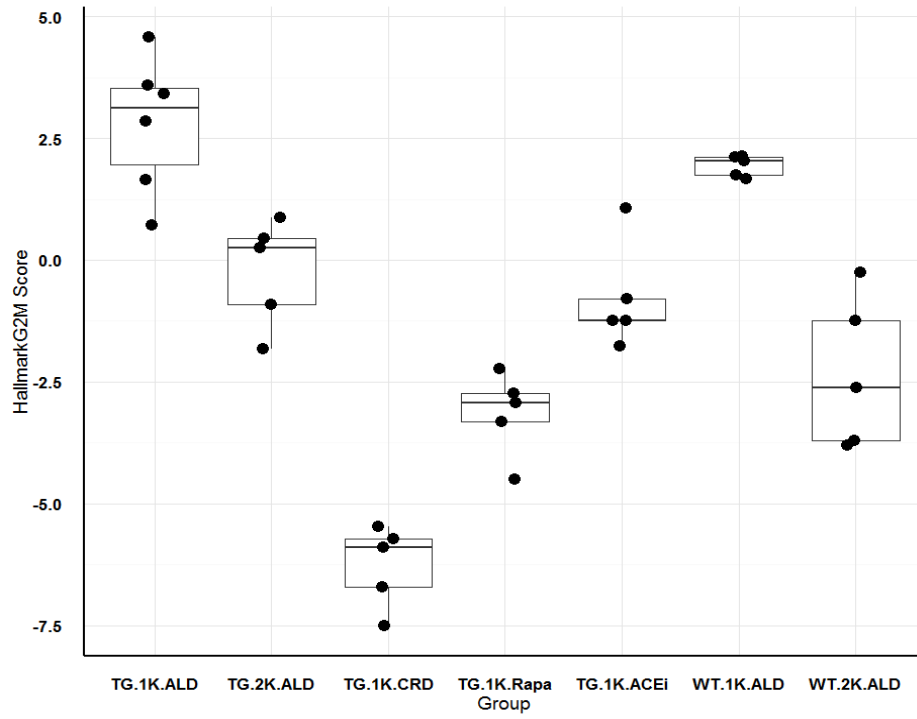


Figure. 7